Atomic Hydrogen Trapped in Solid H$_2$

Dr. James R. Gaines

Department of Physics and Astronomy
University of Hawaii
2505 Correa Road
Honolulu HI 96822

September 1996

Final Report

19961029 089

PHILLIPS LABORATORY
Propulsion Directorate
AIR FORCE MATERIEL COMMAND
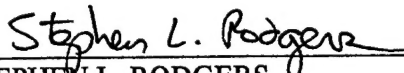**EDWARDS AIR FORCE BASE CA 93524-7048**

DTIC QUALITY INSPECTED 1

NOTICE

When U.S. Government drawings, specifications, or other data are used for any purpose other than a definitely related Government procurement operation, the fact that the Government may have formulated, furnished, or in any way supplied the said drawings, specifications, or other data, is not to be regarded by implication or otherwise, or in any way licensing the holder or any other person or corporation, or conveying any rights or permission to manufacture, use or sell any patented invention that may be related thereto.

FOREWORD

This report presents the results of a study performed by the Department of Physics and Astronomy, University of Hawaii, Honolulu HI 96822 under Contract No. F29601-92-K-0013, for Operating Location AC, Phillips Laboratory (RKS), Edwards AFB CA 93524-7048. The Project Manager for Phillips Laboratory was Dr. Stephen L. Rodgers.

This report has been reviewed and is approved for release and distribution in accordance with the distribution statement on the cover and on the SF Form 298.

STEPHEN L. RODGERS
Director
Propulsion Sciences Division

RANNEY G. ADAMS III
Public Affairs Director

REPORT DOCUMENTATION PAGE

Form Approved
OMB No 0704-0188

1. AGENCY USE ONLY (LEAVE BLANK	2. REPORT DATE September 1996	3. REPORT TYPE AND DATES COVERED Final Report

4. TITLE AND SUBTITLE

Atomic Hydrogen Trapped in Solid H_2

5. FUNDING NUMBERS

C: F29601-92-K-0013

PE: 62601F

PR: 3058

TA: 00FD

6. AUTHOR(S)

Dr. James R. Gaines

7. PERFORMING ORGANIZATION NAME(S) AND ADDRESS(ES)

Department of Physics and Astronomy
University of Hawaii
2505 Correa Road
Honolulu HI 96822

8. PERFORMING ORGANIZATION REPORT NUMBER

9. SPONSORING/MONITORING AGENCY NAME(S) AND ADDRESS(ES)

Phillips Laboratory
OL–AC PL/RKS
10 E. Saturn Blvd.
Edwards AFB CA 93524–7680

10. SPONSORING/MONITORING AGENCY REPORT NUMBER

PL-TR-95-3036

11. SUPPLEMENTARY NOTES

COSATI CODE(S):   2010; 0702; 210902

12a. DISTRIBUTION/AVAILABILITY STATEMENT

Approved for public release; distribution is unlimited

12b. DISTRIBUTION CODE

A

13. ABSTRACT (MAXIMUM 200 WORDS)

The technical work under this contract focused on production and storage of hydrogen atoms in molecular hydrogen hosts. Studies of the diffusion of molecules and atoms in hydrogen hosts were made. In crystalline solids D is controlled by the number of vacancies in the lattice. Values of the parameters used for theory were obtained for all isotopes. Data for the isotopes can be successfully scaled by the quantum parameter.

The atom and molecule hop frequencies were found to be almost identical, making possible the prediction of atom recombination rates. Isotropic substitution has the same effect on the diffusion as increased pressure, but recombination coefficients for crystalline and amorphous solids differ. The anomalous atom growth curves in titrated solids were explained, and a method, based on filling the solid's vacancies, was found for obtaining large atom densities. A new model for in situ atom production for solids containing tritium was developed.

Experiments yielding the diffusion coefficient of HD and H_2 molecules absorbed on activated carbon fibers indicate that these fibers are effective catalysts of the ortho–para transition. Three suggestions are made for future investigation.

14. SUBJECT TERMS

atomic hydrogen; solid hydrogen; quantum theory; hydrogen; atom recombination; HEDM; atomic diffusion

15. NUMBER OF PAGES

56

16. PRICE CODE

.

17. SECURITY CLASSIFICATION OF REPORT	18. SECURITY CLASSIFICATION OF THIS PAGE	19. SECURITY CLASSIFICATION OF ABSTRACT	20. LIMITATION OF ABSTRACT
Unclassified	Unclassified	Unclassified	SAR

CONTENTS

LIST OF FIGURES

LIST OF TABLES

SYMBOLS AND ABBREVIATIONS

ACF	activated carbon fibers
A_0	area per particle
a	nearest neighbor distance
$a\text{-}H_2$	amorphous hydrogen
c	steady-state atom concentration
c_a	concentration of unpaired electron spins
$c\text{-}H_2$	crystalline hydrogen
c_v	probability that any site neighboring a given molecule is vacant
D	diffusion coefficient
D_m	diffusion coefficient for a molecule
D_v	vacancy diffusion coefficient
D_0	diffusion coefficient at infinite temperature
E	initial kinetic energies
EPR	electron paramagnetic resonance
ESR	electron spin resonance
E_a	activation energy
E_b	barrier height
E_t	energy of the first tunneling level
E_v	energy to create a vacancy
fcc	face centered cubic
f_c	correlation function
f_m	tracer correlation factor
FID	free induction decay
H	heat of sublimation
h	Planck's constant
hcp	hexagonal close packed
HEDM	High Energy Density Materials
J_1	splitting of the first tunneling level
K_a	constant rate of atom production
K_1	fit parameter
K_2	fit parameter
L	practical range of a 5.7 keV electron in solid hydrogen
L_0	cylinder length
M	molecule mass
M_2	rigid lattice second moment
N	number density
N_0	Avagadro's number
n	density of atoms
NMR	nuclear magnetic resonance
P	transition probability per unit time
ppm	parts per million
R	rate of conversion from ortho to para

R_c	distance for certain recombination
R_e	range of electron in hydrogen
R_p	peak rate
R_s	transverse dimension of electron trajectory in solid
R_0	cylinder radius
R_β	beta-decay rate
rms	root-mean-square
STP	standard temperature and pressure
T	average recombination time for atoms
t_d	dimensionless time
T_s	scaled temperature
T_{ss}	inverse linewidth from spin-echo experiments
T_{tp}	triple point temperature
T_1	spin-lattice relaxation time
$(T_2)_{RL}$	transverse relaxation time in a rigid lattice
t	time
v	sound velocity
v_0	volume per host molecule
W_{10}	intrinsic conversion rate for an H_2 monolayer
x_a	atom concentration
x_T	tritium concentration
x_v	concentration of vacancies
x_{v0}	equilibrium concentration of vacancies
Z	number of neighbors (12 for hcp)
2-D	two dimensional
3-D	three dimensional
2α	atom recombination coefficient
Γ	atom hop rate
Γ_{any}	rate for an atom to hop to any site
Γ_m	molecular hop rate
Γ_0	rate for a molecule to hop to a vacant neighboring site
ΔH	magnetic field window
$\Delta\omega$	NMR linewidth
ϵ	Lennard-Jones energy scale parameter
Θ	Debye temperature
κ	thermal conductivity
Λ	quantum parameter
ξ_1	constant of order unity
ρ	density
σ	Lennard-Jones length scale parameter
τ_c	correlation time
τ_{hs}	time to hop to a specific site
τ_r	recombination time
τ_d	time needed to diffuse across the bubble radius

Ω intrinsic conversion rate for a fixed atom

Ω_D Debye frequency

SUMMARY

Previous experimental and theoretical work on atoms in solid hydrogen (H_2) leads to the following conclusions: (1) large concentrations of atoms can exist in molecular solids at low temperatures; (2) it is easier to cool samples with known radioactivity than might be imagined; (3) the atoms are inhomogeneously distributed throughout the sample; and (4) application of a magnetic field may increase the concentration of atoms that can be stored at a given temperature or their storage time.

Recent work has focused on maximizing the stored energy in H_2 hosts. These hosts were divided into two categories depending on the method used to form the crystal: crystallization from the liquid phase, c-H_2, or deposition directly from the vapor onto a cold substrate, a-H_2. In both categories of solid H_2, the concentration of metastable particles (atoms) depends on the diffusion coefficient since it controls the recombination rate. Work done under this project can be divided into four areas: (1) quantification of the diffusion and recombination coefficients for three-dimensional (3-D) hydrogen hosts of both c-H_2 and a-H_2 types; (2) development of a new model of the recombination process that predicts observed but previously unexplained atom growth curves and suggests a new approach for obtaining high atom densities; (3) development of a new model for the *in situ* production of atoms in a solid hydrogen host; and (4) new nuclear magnetic resonance (NMR) measurements on hydrogen monolayers on activated carbon fibers that yield the molecular diffusion coefficient for two-dimensional (2-D) hydrogen and an enhanced ortho-para conversion rate.

There are three fertile areas for future investigation. The diffusion coefficients obtained in 3-D hydrogen hosts were for temperatures just below the triple point temperature and for solids crystallized from the liquid state. Extension of these measurements on vapor deposited solids, from the triple point to the lowest possible temperatures, would be very important to the High Energy Density Materials (HEDM) program. In addition, use of non-conventional NMR techniques to extend both sets of measurements to the 5 K vicinity would determine the molecular hopping frequencies unambiguously. The values of the diffusion coefficient obtained for 2-D hydrogen were so large that it is impractical to think of storing metastables in surface layers. These values should be checked because two distinct motional processes can change the width of NMR lines; (1) actual hopping or (2) motion of the spins without hopping. In the latter case, the motional narrowing of the NMR lines does not give information regarding hopping and no conclusion regarding the storage of metastables in surface layers could be drawn from the data.

1.0 INTRODUCTION

The density of energy that can be stored in a host hydrogen solid depends on the diffusion of the metastable particles that carry the energy and that of the host solid. Thus diffusion of metastables in H_2 and that of the host solid molecules is of critical interest to the High Energy Density Materials (HEDM) program.

The work in the HEDM program described in this report concentrated on four aspects of high energy density materials: (1) diffusion of molecules and atoms in 3-D hydrogen hosts; (2) suppression of atomic recombination in H_2 hosts; (3) *in-situ* production of atoms in H_2 hosts; and (4) diffusion of H_2 molecules in 2-D monolayers.

The primary technique for studying H_2 hosts has been nuclear magnetic resonance (NMR), one of the few experimental methods that can study diffusion microscopically since the hopping motion of particles with nuclear spin causes a predictable dephasing of the NMR signal so that the diffusion coefficient can be measured in situ, negating the need for a radioactive tracer element. In addition, cracks (or other extended defects) can actually destroy radioactive tracer experiments but have no effect on NMR experiments. This is true when there is only a small fraction of the diffusing atoms (molecules) in the cracks at any one time since all atoms have equal weight in the NMR signal, independent of their speed.

The solid molecular hydrogens represent an especially interesting class of solids in which to study diffusion since there are three isotopes (H,D, and T) from which molecules with masses of 2, 3, 4 , 5, and 6 can be formed. The molecules are electrically identical so that the intermolecular interactions between the various types of molecules are the same. Since the molecular masses differ, the zero point effects are different, the triple point of H_2 being 14 K while that of T_2 is 20.6 K, leading to very different effective potentials. To date, there have been several experimental investigations pertinent to this work [1-7], but only one theoretical investigation [8] of the molecular self-diffusion coefficient in the solid hydrogens. New data on molecular diffusion is presented and new theoretical models are used to extract the atom diffusion coefficient so that it can be compared with the molecular diffusion coefficient.

1.1 Diffusion in 3-D Hydrogen Hosts

The new NMR data on the molecular diffusion coefficient was taken on the solids HD, D-T, and T_2. This data, combined with existing data on H_2 [1-4], HD [1] and D_2 [5-7], yields a more complete picture of diffusion in the solid hydrogens. The complete set of data is used empirically to obtain the activation energy as a function of isotope mass. A new method is proposed for the temperature scaling of the diffusion data from one isotope to predict the behavior of another.

Comparison of the diffusion coefficients of molecules with those of atoms [9-11] in solid hydrogen, deduced from the data on atomic recombination and obtained from the analysis here and earlier by Souers [12] shows that the diffusion coefficients for atoms and molecules are comparable in the solid hydrogens. This is to be expected if the diffusion of both atoms and molecules is dominated by vacancy exchange. Finally, the scaling used

for the molecular diffusion coefficient is used for the atom diffusion coefficient to predict the diffusion coefficient of T atoms in solid T_2. Calculation of the atomic recombination coefficient in T_2 enables an estimate of the steady-state atom population to be made. This estimate is in good agreement with that inferred from analysis of the ortho-para conversion data [13] in solid T_2.

The diffusion coefficient obtained here is not a directly measured quantity but is deduced from measurements of the damping of NMR spin-echo amplitudes for molecules and the electron spin resonance (ESR) signal loss in time (due to atomic recombination) for atoms. We will review the expressions that will be used to obtain the diffusion coefficients from the data and the Ebner and Sung theory [8] of molecular diffusion in H_2.

1.2 Suppression of Atom Recombination

In analyzing the present results on diffusion, it was found that both atom diffusion and molecule diffusion in the solid hydrogens were dominated by vacancies. Thus when an atom (or molecule) moves by hopping into an available vacancy, it creates another vacancy at the site just left. Using the dependence of the diffusion coefficient, $D(T)$, on the concentration of vacancies, it was concluded that as atoms were created from molecules by the beta decay, the available vacancies would start to fill up since the destruction of one molecule creates one vacancy and two atoms. A quasi-equilibrium theory was obtained to predict the number of vacancies present in solid hydrogen at any temperature as atoms are created from molecules.

1.3 Production of Atoms *In Situ*

Hydrogen solid hosts containing tritium such as T_2, DT, HT, or even H_2, HD, and D_2 doped with some amount of T_2 display very interesting thermal [14] responses such as spontaneous and triggered energy releases and optical properties [15] such as continuous emission and triggered optical pulses at low temperatures. It is known that these solids can store hydrogen atoms but how many of these metastable excitations can exist at any given temperature is still unknown. The atoms stored have their origin in the beta decay of the tritium nucleus. In the gas phase, one beta decay produces about 800 atoms [15] but this number could be different in the solid.

Experiments on such solids have revealed many interesting phenomena. Also, the solids themselves are intrinsically interesting because they represent potential energy storage systems, possibly for space propulsion, and also are the designated cryogenic fuel for inertial confinement fusion experiments. In spite of the great amount of effort spent on some of the quantum aspects of H_2, the materials properties of H_2 are not particularly well known when compared to common substances. To date, there has been little theoretical development of the subject of this report, namely the production of atoms in solid hydrogen due to tritium beta decay although Rosen [16] and Zeleznik [17] did model the unusual thermal responses observed by Webeler [18] on H_2 containing 1% (or less) T_2.

3

1.4 Diffusion in 2-D Monolayers

Pulsed NMR techniques were used to study H_2 and HD molecular monolayers absorbed on activated carbon fibers (ACF) over the temperature range from 4.6 K to 20 K. These fibers have an effective absorption area of 2000 m^2 per gram so that for monolayer coverage, 10^{19} molecules per m^2, 1 gram of ACF holds about 1 liter at standard temperature and pressure (STP) of hydrogen gas. The Fourier transform of the NMR lineshapes, the free induction decay (FID), and the measured height of the FID immediately after the 90° pulse (a quantity that is proportional to the number of spins in the sample) were recorded as functions of time and temperature. The time dependence of the NMR signal in H_2 makes it possible to measure the ortho (spin 1) to para (spin 0) conversion time since only the ortho molecules have an NMR signal. The FID gives the lineshape and enables one to study the spin dynamics of the molecules. Analysis of the NMR data is based on comparisons with that of oH_2-pH_2 mixtures of bulk 3-D solid hydrogen.

2.0 TECHNICAL DEVELOPMENTS

Technical Developments is divided into four sections: (1) diffusion measurements in 3-D hydrogen hosts; (2) suppression of recombination of atoms in 3-D hydrogen hosts; (3) production of atoms *in-situ*; and (4) H_2 monolayers absorbed on activated carbon fibers. In all sections, theoretical advances are included along with the experimental work.

2.1. Diffusion Measurements in 3-D Hydrogen Hosts

To correctly interpret the NMR data, it was necessary to develop a new consistent model of the hop motion of atom and molecules in hydrogen hosts. This model is described below and then used to analyze the data on 3-D diffusion and later the data on diffusion in monolayers of H_2 absorbed on activated carbon fibers.

2.1.1. Theoretical Background. Consider only the monovacancy limit where the concentration of vacancies, c_v, is very small. Let Γ_0 be the basic rate. It is the probability per unit time that a host molecule (e.g., H_2) will hop to a vacant neighboring site. Then the vacancy diffusion coefficient, D_v, the diffusion constant associated with vacancy motion, is:

$$(1) \qquad D_v = \frac{1}{6} Z a^2 \Gamma_0$$

where Z is the number of neighbors, a is the nearest neighbor distance, taken to be the distance of one hop, and 3 is the number of dimensions. For hexagonal close packed (hcp) and face centered cubic (fcc) lattices, $Z = 12$. The probability per unit time that a vacancy will hop is $Z\Gamma_0$ because a vacancy has Z available sites. On average, one-sixth of the jumps take the vacancy in a given direction.

This will be applied to the diffusion of molecules. The probability that any site neighboring a given molecule is vacant (and a molecule can hop to it) is c_v. Thus approximately, the diffusion coefficient for a molecule is $c_v D_v$, though in fact this is not exactly correct since the molecule under consideration and the vacancy can undergo multiple scattering. (For example, the molecule and vacancy could exchange places twice, which would lead to no effect.) The diffusion coefficient for a molecule is written as

$$(2) \qquad D_m = f_m c_v D_v$$

where f_m is the (tracer) correlation factor. It can be shown that

$$(3) \qquad f_m \cong 1 - \frac{2}{Z}$$

and $f_m = 0.781$ for an fcc lattice and certain motions on an hcp lattice.

The molecular hop rate, Γ_m, is defined as $\Gamma_m = c_v Z \Gamma_o = 1/\tau_c$, where τ_c is the correlation time. Except for details like f_m, one can think of Γ_m as the effective hop rate of a host molecule to any site and

$$(4) \qquad D_m = \left(\frac{Z}{6}\right) f_m c_v \Gamma_0 a^2 = \Gamma_m \left(\frac{a^2}{6}\right) f_m$$

It is the hop rate, Γ_m, that Ebner and Sung calculated [8].

Since the data do not yield D directly, it is important to relate D to the measured quantities. The NMR data consist of measurements of the Fourier transform of the NMR lineshapes, the free induction decay, the measured height of the FID immediately after the 90° pulse (a quantity that is proportional to the number of spins in the sample), and the temperature dependence of the NMR time constant (the transverse relaxation time) denoted T_{ss}. This quantity is usually denoted by the symbol T_2 but in this report T_{ss} is used to avoid confusion with molecular tritium in this section. It is roughly equal to the inverse linewidth, from spin-echo experiments. The measured quantity T_{ss} is related to the correlation time, τ_c, by the expression [19] for fcc and hcp lattices:

$$(5) \qquad \frac{1}{T_{ss}} = \left(\frac{M_2}{8.67}\right) b \tau_c$$

where M_2 is the rigid lattice second moment and the pure number, b, depends on the product of the Larmor frequency of the experiment, $\tilde\omega$, and the correlation time τ_c with: b = 38.3, when $\tilde\omega \tau_c \ll 1$ and b = 11.6, when $\tilde\omega \tau_c \gg 1$. All the data taken here are in the latter region, so b = 11.6. Thus $1/T_{ss} = 1.338\, M_2 \tau_c$. Including the factor f_m, the diffusion coefficient for molecules, D_m, will be calculated from the expression:

$$(6) \qquad D_m = \left[1.338\, f_m M_2 T_{ss}\right]\left(\frac{a^2}{6}\right) = \left[1.045\, f_m M_2 T_{ss}\right]\left(\frac{a^2}{6}\right)$$

The net effect of the two corrections on D_m thus amounts to less than 5% when compared to expressions used previously in the literature. The actual lattice spacings for the isotopes [12] are used to calculate D_m from the data.

The single theoretical study pertinent to this work was performed by Ebner and Sung [8]. The Ebner and Sung paper was reviewed and augmented in the paper by Rall, *et al.* [4]. Ebner and Sung considered two possible mechanisms: (1) thermally activated diffusion over a barrier into a vacancy and (2) tunneling through the barrier into a vacancy. The former process would dominate at high temperatures while the latter process would dominate at low temperatures. A diffusion coefficient of the form

$$(7) \qquad D = D_0 \exp\left(-\frac{E_a}{kT}\right)$$

6

was predicted in both temperature regions, with the numerical values of both D_0 and E_a depending on the specific limit. Although Ebner and Sung did not consider the hop of atoms in solid H_2, their results for molecules in H_2 were:

$$\text{(8a)} \qquad D = \left(\frac{a^2}{6}\right)\sqrt{\frac{E_b}{ma^2}}\, \exp\left(-\frac{E_v + E_b - E_t}{T}\right)$$

$$\text{(8b)} \qquad D = \left(6 \times 10^{-4}\ cm^2/s\right) \exp\left(-\frac{197\ K}{T}\right) \qquad [high\ T]$$

$$\text{(9a)} \qquad D = \left(\frac{a^2}{6}\right)\left(\frac{J_1}{\pi}\right) \exp\left(-\frac{E_v}{T}\right)$$

$$\text{(9b)} \qquad D = \left(2 \times 10^{-6}\ cm^2/s\right) \exp\left(-\frac{112\ K}{T}\right) \qquad [low\ T]$$

where m is the mass, E_v is the energy to create a vacancy, E_b is the barrier height, E_t is the energy of the first tunneling level, and J_1 is the splitting of the first tunneling level.

2.1.2 The Diffusion of Atoms. There have been no direct measurements of D for atoms. However measurements of the recombination coefficient can be analyzed to yield the atom hop rate and, hence, the diffusion coefficient. Defining 2α as the atom recombination coefficient, v_0, the volume per host molecule ($a^3/\sqrt{2}$), Z the number of nearest neighbors, τ_{hs} the time to hop to a specific site, τ_r the recombination time, and ξ_1 a constant of order unity, the recombination coefficient can be shown to be equal to:

$$\text{(10)} \qquad 2\alpha = \frac{2Z^2 v_0}{\xi_1 \tau_{hs} + Z\tau_r}$$

If it is assumed that $\xi_1\tau_{hs} \gg Z\tau_r$, then $2\alpha = 2v_0 Z\Gamma_{any}$, where $\Gamma_{any} = Z/\tau_{hs}$, is the rate for an atom to hop to any site and thus Z times larger than the rate to hop to a specific site. The factor Z^2 is obtained because there are Z nearest neighbors to an atom and Z sites leading to each of them. Thus from the recombination coefficient, the atom hop rate is obtained, which can then be compared to the molecular hop rate.

2.1.3 Comparison with Experiment. At the time the Ebner and Sung calculation was completed, NMR data on the diffusion coefficient of H_2, HD, and D_2 existed. Comparison of the theoretical expressions for H_2 and D_2 with existing experimental data gave very good agreement in the high temperature regime but no crossover into the low temperature regime was observed in the data. Ebner and Sung based their comparison with experiment on an analysis of Bloom's NMR data by Moriya and Motizuki [20].

Although the details of their analysis differ from those in this report, Ebner and

Sung obtained the diffusion coefficient for H_2, $D = (2 \times 10^{-3})\exp(-190/T)$ cm^2/s, a result that agreed very well with their prediction. The activation energy of 288 K had been obtained for D_2 from the work of H. Meyer and co-workers [5] and agreed well with that calculated by Ebner and Sung. Thus the activation energies for both H_2 and D_2, obtained from experiment, agreed extremely well with the calculations.

Ebner and Sung did not compare their calculation with the existing data on HD [1]; possibly no calculation was done for HD. Considering how different the existing HD data was from that of H_2 and D_2, it is unlikely that there could have been any agreement. Both the activation energy (E_a) and the prefactor D_0 in HD appear to be anomalous when compared to the H_2 and D_2 values. Bloom comments that there were difficulties in establishing good thermal contact with the HD sample that did not exist for H_2, probably leading to an erroneous determination of the activation energy (and hence D_0) for HD. Since the new experimental values for E_a and D_0 in HD do not appear to be anomalous when compared to H_2 and D_2, they were used and the earlier values were ignored.

The agreement of the Ebner and Sung theory with activation energies and even prefactors obtained from the existing data on H_2 and D_2 appeared excellent since the calculation involved no adjustable parameters. However, if the theoretical result is used to generate numerical values of D in the temperature interval from 14 K to 11 K, the range of the H_2 experiments, and these points are then fitted to Equation 1, one finds $D_0 = 2.8 \times 10^{-5}$ cm^2/s and $E_a = 139$ K, values that do not agree with experiment. This points to a particular problem with the calculation, namely that a crossover to quantum tunneling is predicted about 14.7 K, a temperature just above the triple point of H_2. This crossover has never been observed experimentally in any work on molecules. Since this prediction has never been verified, the quantum part of the Ebner and Sung calculation may be incomplete.

2.1.4 Experimental Data.

New measurements of the molecular self diffusion coefficient in the solid hydrogens have been made by conventional pulsed NMR techniques in T_2, DT, and HD and the original measurements in H_2 have been verified. The new measurements, at 30 MHz, when combined with earlier ones provide a more complete picture of molecular diffusion in these quantum solids and can be interpreted to give some additional insight into the relationship between atomic diffusion and molecular diffusion. The sample configuration, NMR spectrometer, and details of the experimental procedure have been previously published [13].

Experimentally, the temperature dependence of the transverse relaxation time, T_{ss}, in the region where motional effects dominate the observed linewidth was measured. The samples are loaded into the cell as liquids. The temperature is then reduced in increments of about 0.5 K. A Carr-Purcell-Meiboom-Gill pulse sequence was used to measure T_{ss} at the higher temperatures but a single 90° pulse was used when T_{ss} became too short for the longer sequence to be practical. Quadrature detection was used so that the signals had to be phase corrected and then extrapolated to $t = 0$.

All other workers who measured the diffusion coefficient in molecular hydrogen have used the above approach, without quadrature detection, with the exception of the work on D_2 by Meyer and co-workers [6]. They used a more sophisticated approach

involving NMR rotating frame measurements, a technique that is well grounded, theoretically. By comparing their own conventional T_{ss} measurements with the rotating frame measurements, they demonstrated the values obtained by the two techniques agreed (to within experimental error), justifying the usage of the less sophisticated experimental approach used here.

The new NMR measurements of T_{ss} in HD, D-T and T_2 are given in Figure 1. Points taken in the liquid phase are included in this figure but are not included in the analysis of the solid data. The raw data have been converted to calculated diffusion coefficients, $D(T)$, in Figure 2, making it possible to determine the activation energies for all the isotopes. Data taken on the isotopes H_2 and D_2 by H. Meyer and co-workers [5,6] are included for comparison and completeness.
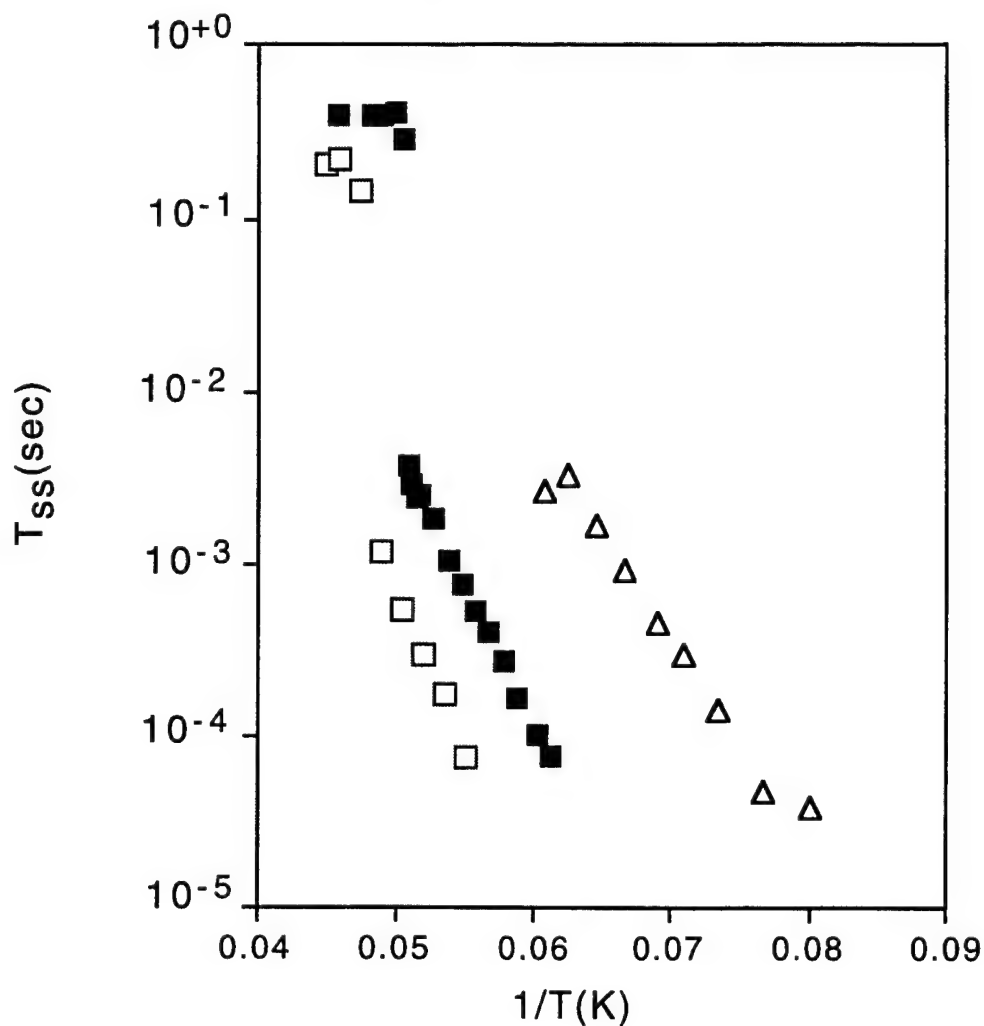

Figure 1
T_{ss} Versus the Reciprocal Sensor Temperature, T^{-1}
The plot symbols are: for HD [Δ]; D-T [■□]; and T_2 [M□].

Points in the liquid phase are shown but not included in the analysis. A temperature correction must be applied to the T_2 and D-T points due to their self-heating.
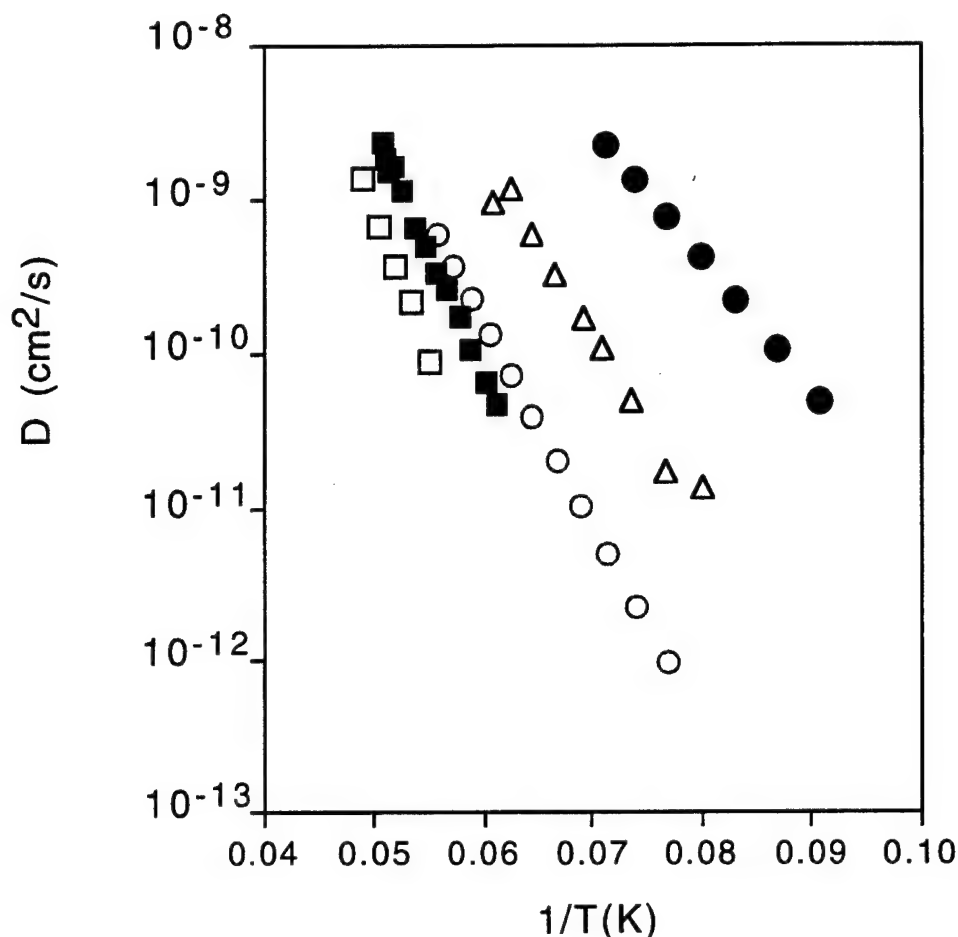

Figure 2
D versus the Reciprocal Sensor Temperature, T^{-1}
The plot symbols are: T_2 [M□], D-T [■], D_2 [V], HD [Δ], and H_2 [v].

One might expect that since the parameters that characterize the 6-12 potential in all the isotopes are the same, the diffusion coefficients should have universal behavior, but they don't. The behavior, while not universal, is smooth, showing only simple thermal activation. Accordingly, Equation 7 was used to fit the data and extract values of E_a and D_0.

Most workers in this field quote D_0 with an error of ±100% because of the approximate nature of the expressions used to calculate D_0. Moreover, a small error in E_a can make a big change in D_0. There are additional problems in radioactive samples. There, temperature gradients exist in the solid due to the heating resulting from the beta decay of the triton. The results presented here are corrected for these gradients and average temperatures are quoted. Still, these gradients can lead to an error of three to five

in D_0. The temperature correction is discussed in detail.

For both T_2 and D-T, the sensor temperature is not necessarily equal to the average sample temperature. In the experiments, the volume of the samples were: 0.167 cm^3 for T_2 and 0.172 cm^3 for D-T. These numbers are based on use of 200 cm^3 of gas at STP. The sapphire cell (a cylinder) had an inside diameter of 0.762 cm, making the thickness 0.366 cm for T_2 and 0.377 cm for D-T. Thus the sample radius is approximately equal to the thickness. Heat could be removed from the bottom or radially, or both. Unfortunately, hydrogen samples have a tendency to pull away from walls as they are cooled below the triple point so it is not certain that the sample remained in contact with the walls. The temperature correction will be estimated in the best case, where the sample remains in contact with the walls and in the worst case where the sample pulls away from the walls.

Based on molar volumes of 18.75 x 10^{-6} m^3/mol for T_2 and 19.29 x 10^{-6} m^3/mol for D-T, the samples generated 1.745 x 10^{-2} W (T_2) and 8.723 x 10^{-3} W (D-T). Using the thermal conductivity values from Collins *et al.* [17], with 0.35 W/mK for T_2 and 0.30 W/mK for D-T as representative values, the average temperatures for the best case (both radial and vertical heat flow) are given by:

T_2: $T_{avg} = T_{sensor} + 0.488$ K
D-T: $T_{avg} = T_{sensor} + 0.237$ K

For the worst case, $T_{avg} = T_{sensor} + HL^2/3k$, where H represents the self-heating and k is the thermal conductivity (with L the length) giving

T_2: $T_{avg} = T_{sensor} + 0.666$ K
D-T: $T_{avg} = T_{sensor} + 0.343$ K

Using these corrections, it is now possible to obtain the activation energies and the appropriate error bars. Measurements on DT between the temperatures, 21.6 K and 16.1 K, yield $E_a = 372$ K and $D_0 = 0.34$ cm^2/s. Measurements on T_2 between the temperatures, 21.7 K and 17.7 K, yield $E_a = 432$ K and $D_0 = 1.8$ cm^2/s. The activation energies for T_2 and D-T are based on the best case heat removal. If error bars are derived by using the worst case scenario, one has for T_2, $E_a = 432$ K ±20 K and D-T, $E_a = 372$ K ±10 K.

Additional errors come from the measurement error in the quantity T_{ss} used in Equation 6 to calculate D. Because of the very high signal-to-noise ratio in the experiments, the error in determining T_{ss} is less than $\pm5\%$. Calculated values of M_2 were used in Equation 6, and since these values depend on the nearest neighbor spacing (a), the value of D depends on (a)$^{-4}$. The error in this quantity was neglected since the molar volumes are known to be better than 1%. In addition, the errors in the measurement of temperature where it is measured and regulated to better than 50 mK at 20 K have been neglected. Thus the values of D calculated from Equation 6, due to random errors in T_{ss}, are uncertain to $\pm5\%$. For extreme cases, this also translates into an error in the activation energy of $\pm5\%$, also. Combining the two sources of error for T_2 and D-T one obtains for T_2, $E_a = 432$ K ±42 K and D-T, $E_a = 372$ K ±29 K. A random error in E_a of $\pm5\%$ can introduce an error in D_0 of a factor of 2 or 3. Thus the values of D_0 obtained

here are only order of magnitude estimates. They are listed below to two significant figures to make it possible to calculate individual values of D to within 10%.

Measurements on H_2 and HD were repeated. The results on H_2 agreed well with the earlier data of Bloom [1] and Weinhaus and Meyer [3] and the more recent measurements by Rall *et al.* [4]. The new results on HD disagree completely with the early results of Bloom [1]. For measurements between T = 12.5 K and T = 17.1 K, the new data yields E_a = 250 ±12 K and D_0 = 5.4 x 10^{-3} cm^2/s (correct to within a factor of 2 or 3). The results obtained here and selected results of other workers are given in Table I [18].

Table 1. The Activation Energies and Diffusion Coefficient Prefactors for Molecules

Isotope	E_a(K)	H(K)	D_0(cm^2/s)	Λ
H_2	197 [3]	92.6	2.8 x 10^{-3}	1.731
HD in H_2	197 [4]		5.7 x 10^{-3}	
HD	250	116.7	5.4 x 10^{-3}	1.471
D_2	300 [7]	138.3	1.0 x 10^{-2}	1.224
D-T	372	150.3	0.34	1.111
T_2	432	164.8	1.8	1.00

For reference, the heat of sublimation, H(K), and the quantum parameter (Λ), defined in Equation 11, are included.

2.1.5 Analysis and Interpretation. In this section data taken on molecules and atoms in the solid hydrogens will be analyzed and interpreted. Some of the samples were made by slow crystallization from the liquid phase while others were formed by deposition of vapor on a cold substrate.

In attempting to compare data on molecules in different quantum solids, it is customary to use reduced variables, an approach similar to that used in applying the law of corresponding states to the behavior of different gases in an attempt to see the universal features of all gases. The reduced variables in this case are formed from dimensionless combinations obtained from the two Lennard-Jones parameters, ϵ and σ [15]. Unfortunately, these parameters are approximately the same for all the hydrogen isotopes so that one prediction of this approach would be that the product of the diffusion coefficient (D) and the square root of the mass ($\sqrt{m}$) would be the same for all the hydrogen isotopes. This is clearly incorrect for the data in Figure 2. For instance, by

12

drawing a horizontal line, it can be seen that the same values of D occur for widely different values of $1/T$ or, for a given value of T, the diffusion coefficient of the lightest isotope, H_2, is far larger than that of the heaviest isotope, T_2. This is a clear quantum effect. A different method of comparing the isotope data is required.

What was needed was a non-trivial temperature scaling so that it could be determined how the parameters D_0 and E_a vary from isotope to isotope, even though the potentials are essentially the same, except for the equilibrium spacings of the molecules. One method that works is temperature scaling based on the quantum parameter [15]. The basic idea is shown in Figure 3 where the triple point temperature (T_{tp}) of each isotope, multiplied by the quantum parameter for that isotope, is plotted as a function of the quantum parameter, Λ, where

$$(11) \qquad \Lambda = \left[1 + \frac{1}{6} \frac{(M_a - M_b)^2}{M_a M_b} \right]^{1/2} \frac{N_0 h}{\sigma (M \epsilon)^{1/2}}$$

where N_0 is Avogadro's number, h is Planck's constant, σ and ϵ are the Lennard-Jones parameters, and M_a and M_b are molecular weights of the atoms in the molecule (for heteronuclear molecules), with M being the molecular weight of the molecule. The product ΛT_{tp} is roughly constant with a mean value of 22.8 and an rms deviation of 6% even though the triple point temperatures range from 13.8 for H_2 to 20.6 for T_2. Since the triple point temperature (essentially an energy) scales as $1/\Lambda$, the same Λ dependence for the activation energy is expected. The product $E_a \Lambda/16$ is plotted in Figure 3. The product $E_a \Lambda$ is constant to within 10%.
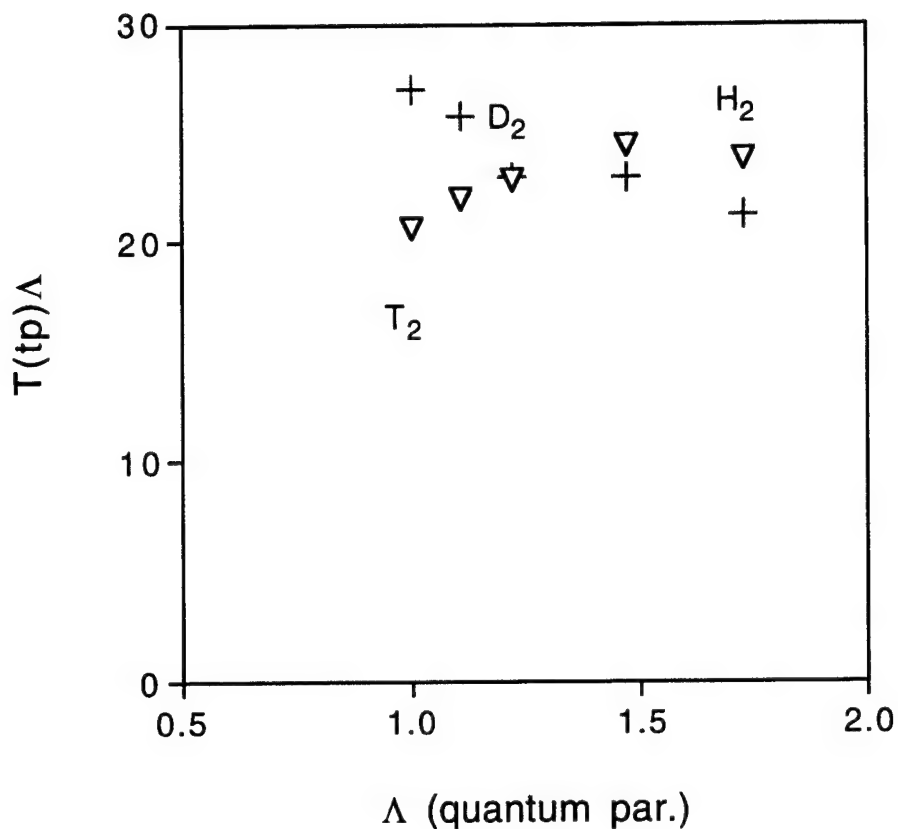
Figure 3

$T_{tp} \Lambda$ and $E_a \Lambda$ versus Λ

This approach to scaling is illustrated in Figure 4, where the diffusion coefficients for all the isotopes are plotted as a function of $[T\Lambda]^{-1} = 1/T_s$, where T_s is the scaled temperature. The data for all the isotopes fall on essentially parallel lines indicating the temperature scaling is adequate but the prefactors, D_0, are all different and no suitable method for scaling them has been found although the non-radioactive isotopes appear to be regular and the radioactive isotopes are anomalous.
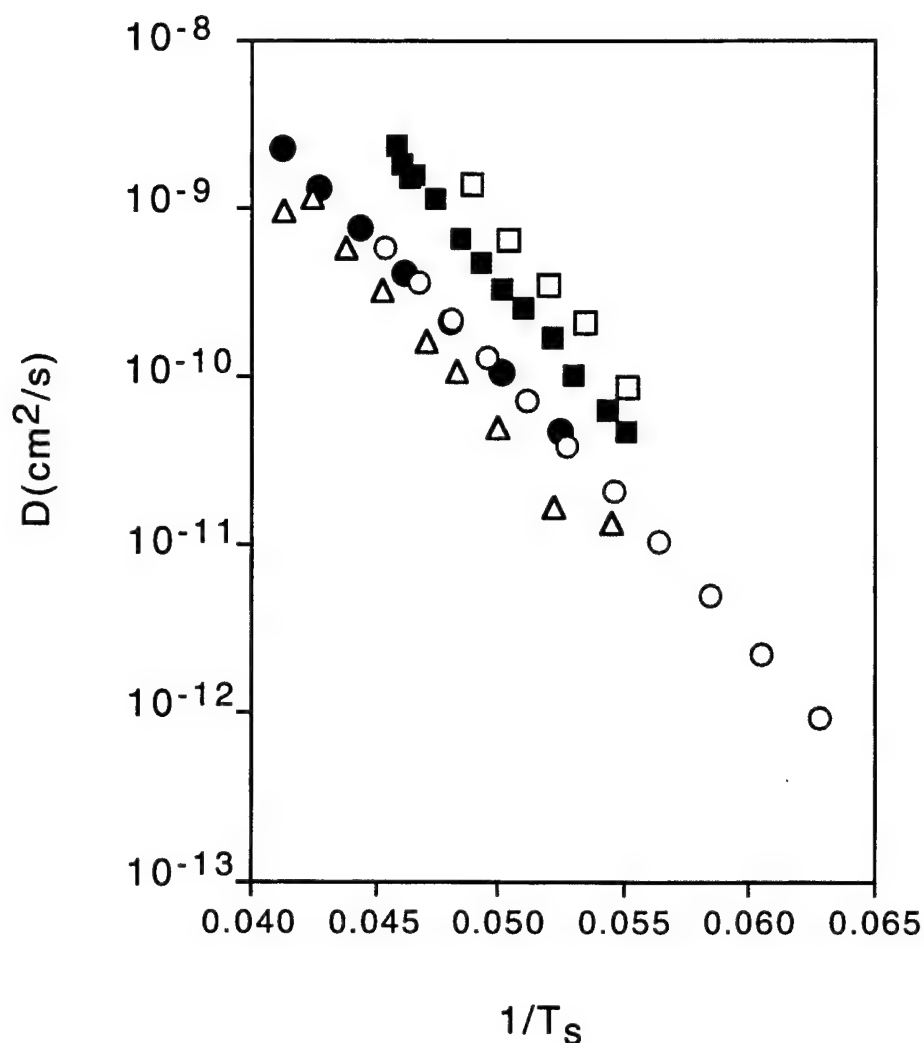
Figure 4
D versus $T_s = T\Lambda$

The plot symbols are: T_2 [M□], D-T [■□], D_2 [V], HD [Δ], and H_2 [v].

The measured activation energy, at high temperatures, is composed of three terms, according to Ebner and Sung [8], $E_a = E_v + E_b - E_t$, where E_v is the vacancy energy, E_b is the barrier energy, and E_t is the energy of the first tunneling level. By suitable modeling, it is possible to estimate the three contributions individually. Ebner and Sung calculated the lowest energy level in the potential well for H_2 and obtained the value of $E_t = 34.1$ K, a value they also used for D_2. If the shape of the well doesn't change appreciably, then the energy levels for the other isotopes should be simply obtained from the hydrogen value, namely $E_t \propto \Lambda$, where Λ is the quantum parameter (since the harmonic oscillator energy depends on $1/\sqrt{m}$. Thus the tunneling energies are: H_2 (34.1 K); HD (29.0 K); D_2 (24.1 K); D-T (21.9 K); and T_2 (19.7 K).

The energy to form a vacancy in a perfect, non-quantum solid hydrogen is 210 K [21] and quantum effects should reduce this value proportional to $1/\sqrt{m}$; hence, a power

15

series in the quantum parameter is suggested. Keeping only the first three terms,

$$(12) \qquad E_v = 210\ K - K_1(\Lambda) + K_2(\Lambda)^2$$

Ebner and Sung gave the values of 112 K and 132 K for H_2 and D_2 so both K_1 and K_2 can be determined. This yields the values, $E_v = 112$ K, 121 K, 132 K, 137 K, and 143 K for H_2, HD, D_2, D-T, and T_2, respectively. There is no information about the values for HD, D-T, or T_2 in the literature.

For E_b, there appears to be no theoretical guideline similar to the one used for E_v. The experimental value of E_a, the calculation of E_t and the fit to E_v, are used to obtain values of $E_b = E_a + E_t - E_v$ for all the isotopes. Ebner and Sung calculated $E_b = 119$ K and 192 K for H_2 and D_2. The values obtained in this manner are: $E_b = 119$ K, 158 K, 192 K, 257 K, and 309 K for H_2, HD, D_2, D-T, and T_2, respectively.

From the determination of the hop frequencies for the isotopes, it is possible to calculate the hop frequency of a vacancy at the triple point for comparison. All the solid hydrogens have about the same Debye temperature, approximately 100 K. This translates into a Debye frequency of $(\Omega_D) = 1.31 \times 10^{13}$ s^{-1}, four orders of magnitude larger than the vacancy hop frequency at the triple point temperature, as seen below.

To extract the hop frequency of vacancies, at the triple point, for H_2 one uses the expression:

$$(13) \qquad \left(\Gamma_{any}\right)^{H_2} = 12\ c_v \Gamma_0 = 12\ \Gamma_0 \exp\left(-\frac{E_v}{T}\right)$$

Solving for Γ_0 using values of E_v taken from best fit gives, yields at the triple points:

$\Gamma_0 = 2.75 \times 10^9$ s^{-1} for H_2 using triple point temperature of 13.8 K.
$\Gamma_0 = 1.08 \times 10^9$ s^{-1} for HD using triple point temperature of 16.6 K
$\Gamma_0 = 0.62 \times 10^9$ s^{-1} for D_2 using triple point temperature of 18.7 K
$\Gamma_0 = 1.21 \times 10^9$ s^{-1} for D-T using triple point temperature of 19.8 K
$\Gamma_0 = 0.86 \times 10^9$ s^{-1} for T_2 using triple point temperature of 20.6 K.

Thus to within a factor of 4, the vacancy hop rate, at the triple point temperature, is the same for all the hydrogen isotopes.

The hopping of atoms controls the steady-state atom population trapped in solid hydrogen. This has never been studied directly through a measurement of the atom diffusion coefficient but there are two other approaches that have probed the steady-state atom population and the atom dynamics. These are ESR studies and measurements (and modeling) of the ortho to para conversion of molecules of T_2 in solid T_2. In this case, there have been measurements on crystalline solids and also measurements on amorphous solids.

Leach and Fitzsimmons [9] produced H atoms in crystalline H_2 by electron bombardment and studied atom recombination after the electron beam was turned off.

Defining n to be the atom density, after the beam is off,

$$(14) \qquad \frac{dn}{dt} = -(2\alpha)n^2$$

where 2α is the atom recombination coefficient. They could measure it directly from the time decay of the ESR signal, which was proportional to the density of atoms, n. They found that

$$(15) \qquad \alpha = \alpha_0 \exp\left(-\frac{E_a}{T}\right)$$

where the activation energy $E_a = 195 \pm 10$ K, remarkably like that found for H_2 molecules in solid H_2. The relationship between the recombination coefficient and the atom hop rate (Γ), Equation 10, can be used to extract Γ from the measured values of α. After setting the activation energies to a common value, it is found that

$$(\Gamma)^H = (5.9 \times 10^{13} \text{ sec}^{-1})\exp(-197/T)$$

This can be compared with the molecular hop rate obtained from the NMR data

$$(\Gamma)^{H2} = (1.56 \times 10^{13} \text{ sec}^{-1})\exp(-197 \text{ K}/T)$$

showing that the atom and molecule hop rates are almost identical in H_2, differing only by a factor of 4.

Other important information about crystalline solids is provided by the data taken using NMR techniques on the ortho to para conversion in solid T_2 [13]. There have been no direct measurements of the atom recombination coefficient in solid tritium. Because the ortho-para conversion process is catalyzed by the presence of atoms [13], the rate is a sensitive function of the steady-state atom population. Using this fact, one can extract the atom recombination coefficient from that data and calculate the atom hop rate, also.

Defining R to be the rate of conversion from ortho to para, one obtains:

$$(16) \qquad R = \frac{c\Gamma\Omega}{\Gamma + \Omega}$$

where c is the steady-state atom concentration, Γ is the atom hop rate and Ω is the intrinsic conversion rate for a fixed atom [13]. The conversion rate has a sharp maximum near 10 K, yielding a peak rate $R_p = 8 \times 10^{-4}$ s^{-1}. The concentration, c, is found from the equation

$$(17) \qquad c = N_a/N_T = [K/2aN_T^2]^{1/2}$$

17

By dividing R in Equation 16 by the peak rate, one obtains a simple function of the ratio of Γ/Ω, namely $R/R_p = 2(\Gamma/\Omega)^{1/2}/[1 + \Gamma/\Omega]$. Defining $x^2 = \Gamma/\Omega$, the value of x can be obtained as the solution of a quadratic,

$$(18) \qquad x = R_p/R \pm \sqrt{[(R_p/R)^2 - 1]}$$

The ratio Γ/Ω can be obtained at each temperature. The value of Ω is obtained from the peak rate and this sets the scale for the hop rate also. The values of Γ obtained by this analysis are given in Table 2. The recombination coefficient is then calculated from Γ, using Equation 10 in the form $2\alpha = 2v_0 Z \, \Gamma$.

Table 2. The Atom Hop Rate (Γ), Extracted from the Ortho-para Conversion Rate in T_2, its Reciprocal (τ), and the Atom Concentration (c) in Parts Per Million (ppm), Tabulated at Various Temperatures

T(K)	R(s^{-1})	R$_p$/R	Γ/Ω	Γ (s^{-1})	τ (sec)	c$_a$ (ppm)
6	1.11E-04	7.2100E+00	4.86E-03	4.39E-02	2.28E+01	2.54E+03
6.4	1.23E-04	6.5000E+00	6.00E-03	5.42E-02	1.84E+01	2.28E+03
7.9	1.72E-04	4.6500E+00	1.20E-02	1.08E-01	9.22E+00	1.62E+03
9.5	2.87E-04	2.7900E+00	3.40E-02	3.07E-01	3.25E+00	9.60E+02
10.6	5.42E-04	1.4800E+00	1.51E-01	1.37E+00	7.31E-01	4.56E+02
10.7	5.62E-04	1.4200E+00	1.70E-01	1.53E+00	6.52E-01	4.29E+02
12.6	3.32E-04	2.4100E+00	2.12E+01	1.92E+02	5.22E-03	3.84E+01
14	1.12E-04	7.1400E+00	2.02E+02	1.83E+03	5.48E-04	1.25E+01
15	8.32E-05	9.6200E+00	3.68E+02	3.33E+03	3.01E-04	9.20E+00

In Figure 5, the recombination coefficient obtained by ESR techniques for H atoms in crystalline H_2 is plotted for comparison with the T atom recombination coefficient obtained by modeling the NMR data on solid T_2. The temperature is scaled by the quantum parameter for H_2, namely $\Lambda = 1.731$ since $\Lambda = 1$ for T_2.
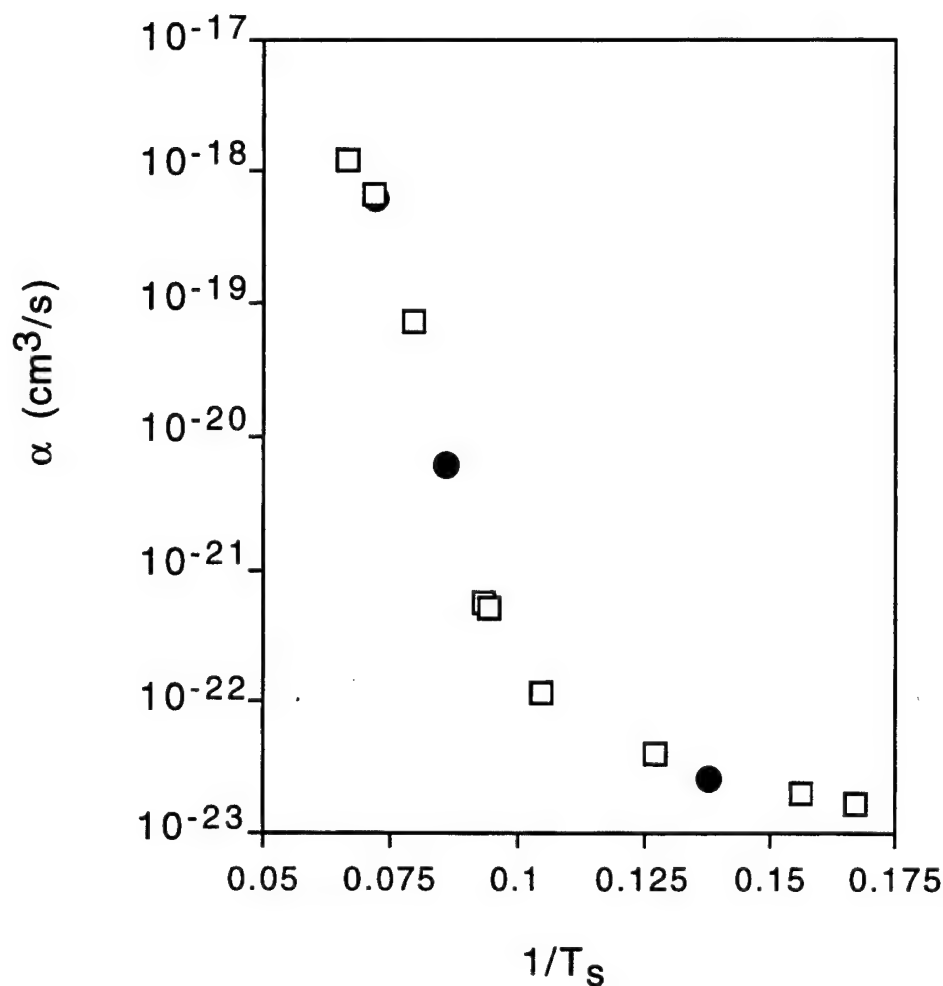
Figure 5

α Versus T_s^{-1}

The plot symbols symbols are: T_2 [M□] and H_2 [v].

The agreement is outstanding even though the recombination coefficients are no longer following a simple thermally activated form.

The data taken in Russia on atoms in H_2 and D_2 [9,10] represent data on amorphous, not crystalline solids. Up to now there has been an attempt to understand the two sets of data in terms of the extensive database that exists on the crystalline hydrogens. A different approach will be used here. Their samples were prepared by depositing streams of H_2 or D_2 gas, containing atoms produced by microwave discharge, onto cold substrates, held at 2 K or below. The recombination coefficients for the amorphous samples are compared in Figure 6 with those from crystalline samples. Note that there is not good agreement even between the amorphous H_2 and D_2 experiments, nor is there agreement between the amorphous and crystalline samples. There remains the possibility that the samples never reached equilibrium and the vacancies were not thermal vacancies.

19
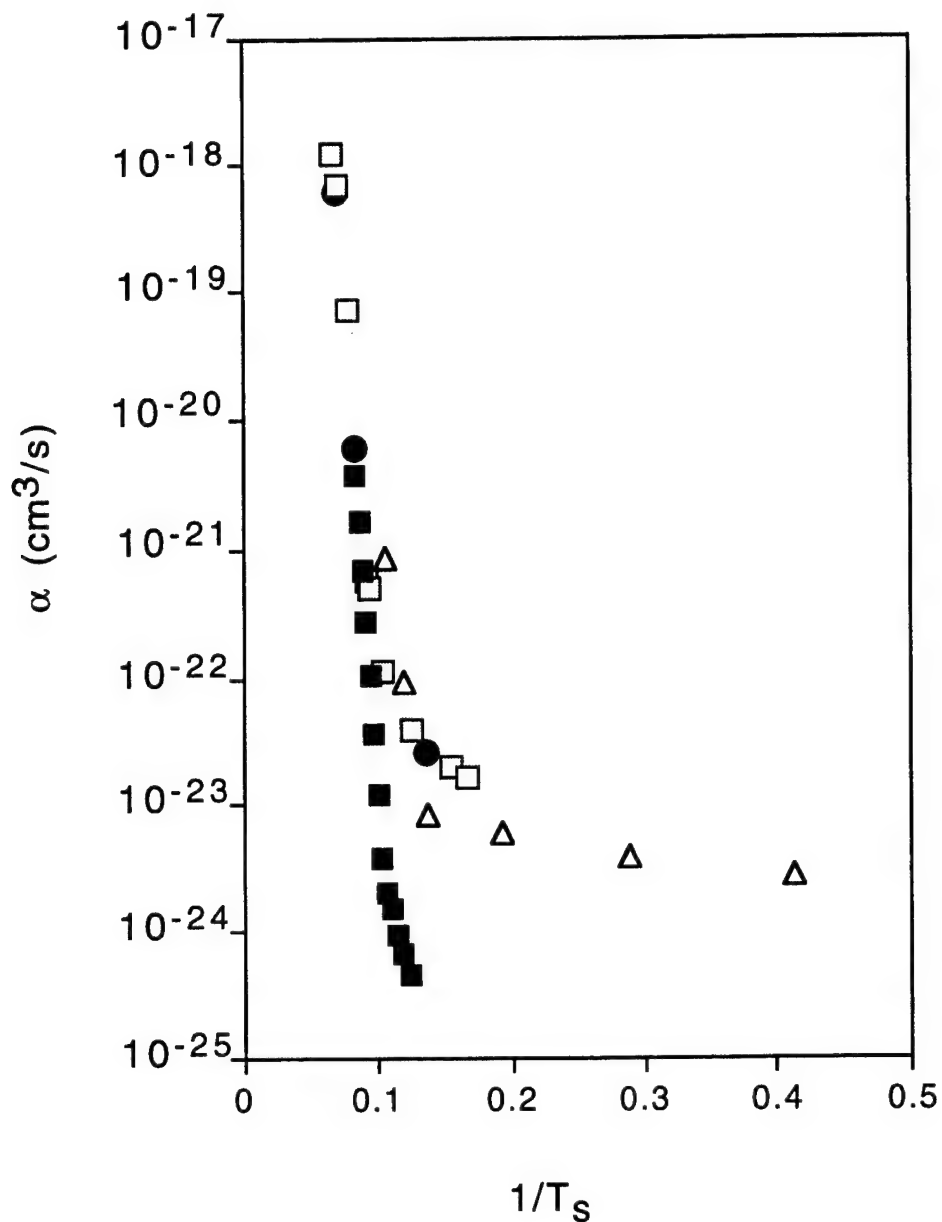
Figure 6
α Versus T_s^{-1}

2.2. Suppression of Recombination of Atoms in 3-D Hydrogen Hosts

In its simplest form, the diffusion coefficient D can be written as:

$$(19) \qquad \qquad D(T) = D_0 x_v$$

where D_0, at low temperatures, would be the diffusion coefficient appropriate for activation over the potential barrier between molecules and x_v is the concentration of vacancies. As a first approximation, it is found that $x_v = x_{v0} - (\frac{1}{2})x_a$ where x_{v0} is the initial concentration of vacancies at a given temperature and x_a is the concentration of atoms.

20

Thus $D(T) = D_0(x_{v0} - (\frac{1}{2})x_a)$ so that as the atom concentration increases, the diffusion coefficient (and hence the recombination coefficient) decreases, making larger atom populations possible. Using this modified value for the diffusion coefficient leads to very large differences in the interpretation of experimental results. Specifically, it predicts that (1) the atom growth at a given temperature can have the shape observed in electron paramagnetic resonance (EPR) experiments of Sharnoff and Pound [22] and later by Collins [23]; and (2) atom populations larger that the above calculated steady-state values can be obtained. The strange atom growth feature has defied explanation for 30 years, until now.

The theoretical work reported here, done in collaboration with Dr. Peter Fedders, Department of Physics, Washington University, has produced a breakthrough in the understanding of the kinetics of the atom growth in solid hydrogen containing tritium. The tritium undergoes a beta decay with a rate that is almost constant over the life of an experiment since the decay half-life is 12.3 years.

The electron emerging from the beta decay loses its energy by ionizing and/or exciting hydrogen molecules in its path, producing atoms of hydrogen. If the same processes occurred in the solid as are observed in the gas, each beta decay would produce about 1000 atoms. These atoms, once produced, are metastable and decay (through recombination into molecules) with other atoms. Since the production of atoms via the tritium beta decay is constant in time, recombination limits the atom population and, in the simplest of cases, a steady-state population of atoms results. This simple case is not always observed and, recently, insight was obtained into the process that may make it possible to maintain larger populations of atoms than previously thought.

If n is defined to be the atom density (number of atoms per cm^3), then the simplest rate equation describing the production and recombination of atoms is:

$$(20) \qquad\qquad \frac{dn}{dt} = K_a - (2\alpha)n^2$$

where K_a is the constant rate of atom production in atoms per second per cm^3. This is a known quantity and can be calculated from the beta-decay rate: $R_\beta = 1.14 \times 10^{14} (x_T)$ decays per cm^3 per second; where x_T is the tritium concentration in the sample; and the number of atoms produced per beta decay, approximately 1000; yielding $K_a \approx 1.14 \times 10^{17} (x_T)$ atoms/cm^3/s. The recombination coefficient, written as 2α, is another matter. It has been measured directly in only one experiment and is less well understood. In a graph of n versus time (t), starting from $n = 0$ at $t = 0$, the atom growth curve, the above expression predicts that:

$$(21) \qquad\qquad n = n_0 \tanh\left(\frac{t}{\tau}\right)$$

where n_0 is the steady-state value of the atom density, $n_0^2 = K_a/2\alpha$ and $\tau = 1/\sqrt{2\alpha K_a}$. The predicted growth curve is smooth beginning at zero and saturating at the value n_0.

21

The two experiments [22,23] that have observed growth curves that are very different from the predicted curve both found a distinct plateau in the curve after an initial buildup followed by a second region of atom growth. This behavior is shown in Figure 7.
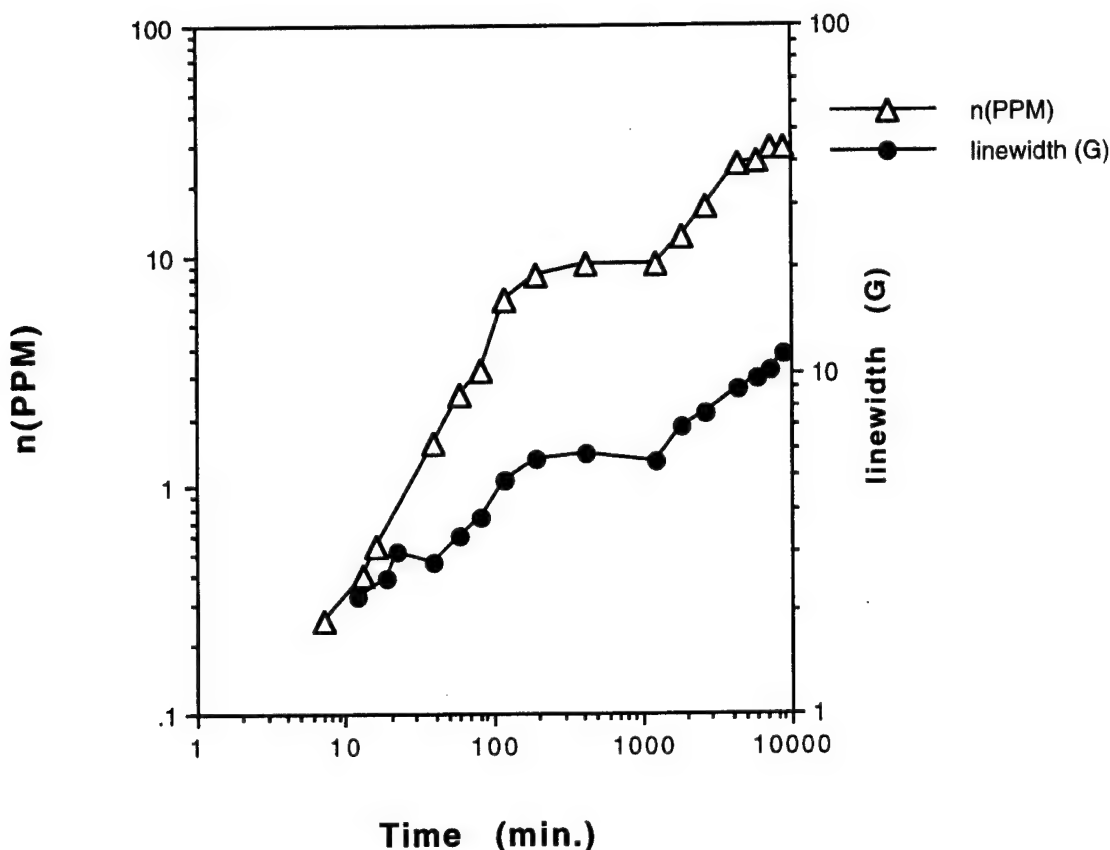
Figure 7
Atom Density as a Function of Time

One approximate form for the recombination coefficient is $2\alpha = 4\pi R_c D(T)$, where R_c is the distance (from another atom) where recombination is certain (usually taken to be the lattice spacing) and $D(T)$ is the diffusion coefficient for an atom. Since $D(T)$ is determined by the vacancy motion, filling of the vacancies reduces the recombination coefficient making the second atom buildup, after the initial plateau, possible. This model, without the feature of vacancy filling, has been previously used to describe the crudest features of atom dynamics, namely constant production (K_a) and temperature dependent two-particle recombination.

This simple rate expression agrees in its time dependence, when $K_a = 0$, with the only direct measurement [9] of the recombination coefficient (2α). This simple expression predicts that the atom density increases as the hyperbolic tangent and saturates. It cannot yield a time dependence such as that seen by Sharnoff and Pound [22] and also by Collins [23] under a variety of conditions. Such a time dependence is characterized by an

22

inflection point in the curve of n(t) versus t. Thus the second derivative of n(t) versus t must be equal to zero at an inflection point.

Making the simple modification of equating the recombination coefficient (2α) to $(2\alpha)_0 x_v$, where x_v is the concentration of vacancies, produces a rate equation that has an inflection point and can, at least crudely, describe the observed atom time dependence. The concentration of vacancies is roughly given by: $x_v = x_{v0} - x_a/2$, where x_a is the atom concentration given by n/N with N the number density of molecules and x_{v0} the equilibrium concentration of vacancies. Introducing this into the initial rate equation gives:

(22)
$$\frac{d(Nx_a)}{dt} = K_a - (2\alpha)_0 \left[x_{v0} - \frac{1}{2} x_a \right] x_a^2 N^2$$

The second derivative is zero when $x_a = (4/3)x_{v0}$. The steady-state solution of this cubic equation is:

(23)
$$x_a^3 = 2x_{v0} \left[x_a^2 - \left(\frac{n_0}{N} \right)^2 \right]$$

where $n_0^2 = K_a/(2\alpha)_0 x_{v0}$, the atom density that would be obtained in the steady-state if atom production didn't fill the vacancies and inhibit diffusion and recombination.

If $x = x_a/x_{v0}$ and $x_0 = n_0/Nx_{v0}$ are defined, then the above condition for a steady-state solution becomes:

(24)
$$x^2 - \frac{1}{2} x^3 = x_0^2$$

The right hand side is always positive and the left hand side can be positive on the interval $x = 0$ to $x = 2$, the inflection point being at $x = 4/3$. The maximum difference between the two terms on the left hand side is 16/27, also occurring at $x = 4/3$. Thus depending on the ratio of the saturation concentration of atoms to the concentration of vacancies, there can be a steady-state solution for $x < 4/3$. For such a solution, the atom concentration will be approximately equal to (or less than) the vacancy concentration.

There is one important implication of this simple result: the larger the number of vacancies, the higher the atom concentration, in the steady-state or at the beginning of a non-equilibrium buildup where there is an inflection point. This point is new and has strong implications for preparing hydrogen solid to hold the maximum number of atoms.

When the quantity x_0 is very small, a steady-state solution is possible with $x = x_0$. The quantity x_0 is very temperature dependent, as seen from the expression:

$$(25) \qquad x_0^2 = \frac{K_a}{(2\alpha)_0 x_{v0}^3 N^2}$$

thus at higher temperatures, a steady-state solution could exist. At lower temperatures x_0^2 could exceed its critical value of 16/27 and no steady-state solution would exist, only an inflection point and a monotonically increasing atom concentration.

By defining a dimensionless time, $t_d = [N(2\alpha)_0 x_{v0}^2]t$, the rate equation becomes:

$$(26) \qquad \frac{dx}{dt_d} = x_0^2 - x^2 + \frac{1}{2} x^3$$

which is integrable. The time dependence predicted by this equation is shown in Figure 8. Note, when x_0 exceeds the critical value, the time dependence predicted is that seen by Sharnoff and Pound [22]. In this figure, the value of x_0^2 is taken to be (16.1/27), just above the critical value of (16/27). When the term that takes vacancy filling into account is omitted, the scaled concentration (x) increases uniformly and then saturates at about x = 0.77. When vacancy filling is taken into account, the scaled concentration increases uniformly to a much larger plateau value before a runaway region of increase.
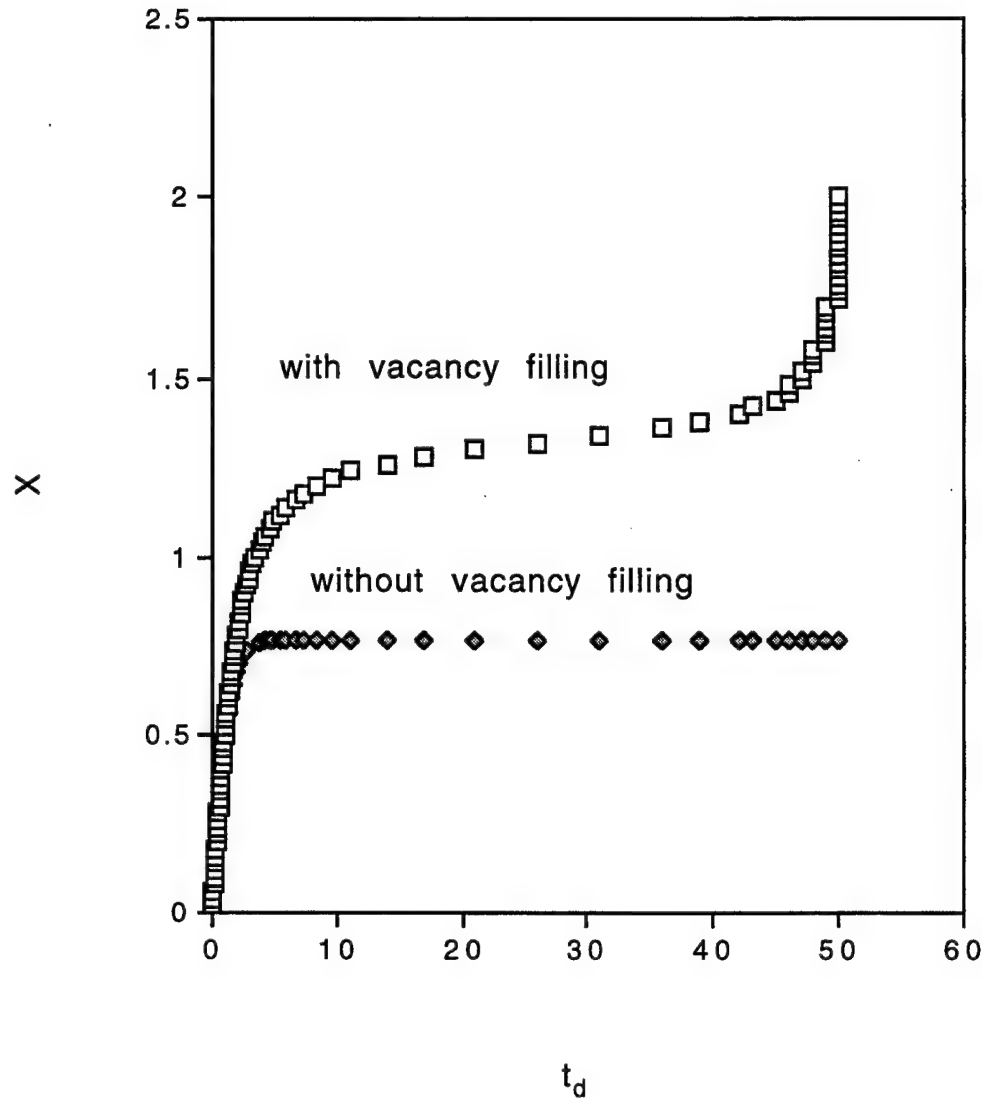
Figure 8
The Predicted Concentration versus Dimensionless Time

The right-hand side of Equation 26 can be defined to be $B(x)$. $B(x)$ has a minimum at $x = 4/3$, independent of x_0, as can be seen in Figure 9. When $x_0^2 = (16/27)$, the minimum value is exactly zero so this value is the critical value. The points where $B(x) = 0$ are called fixed points. They become singularities of the following integral and are the limiting values of the solutions to the differential equation for the atom concentration.

$$(27) \qquad t_d = \int_0^x \frac{dx'}{B(x')}$$

When $x_0^2 < (16/27)$, the solution, starting at $x = 0$, proceeds smoothly to the first turning point, the smallest root, x_1, on the positive x axis of the cubic equation $0 = x_0^2 - x^2 + 0.5$

25

x^3. In simple terms, the atom concentration would build smoothly and then saturate at the value x_1. It is interesting to note that the value of x_1 depends on x_0. When $x_0^2 = (16/27)$, the value of x saturates at x = 4/3. This model is capable of explaining the time dependence seen by Sharnoff and Pound [22] and predicts that more metastable particles can be trapped in a solid by filling the vacancies and reducing the diffusion.
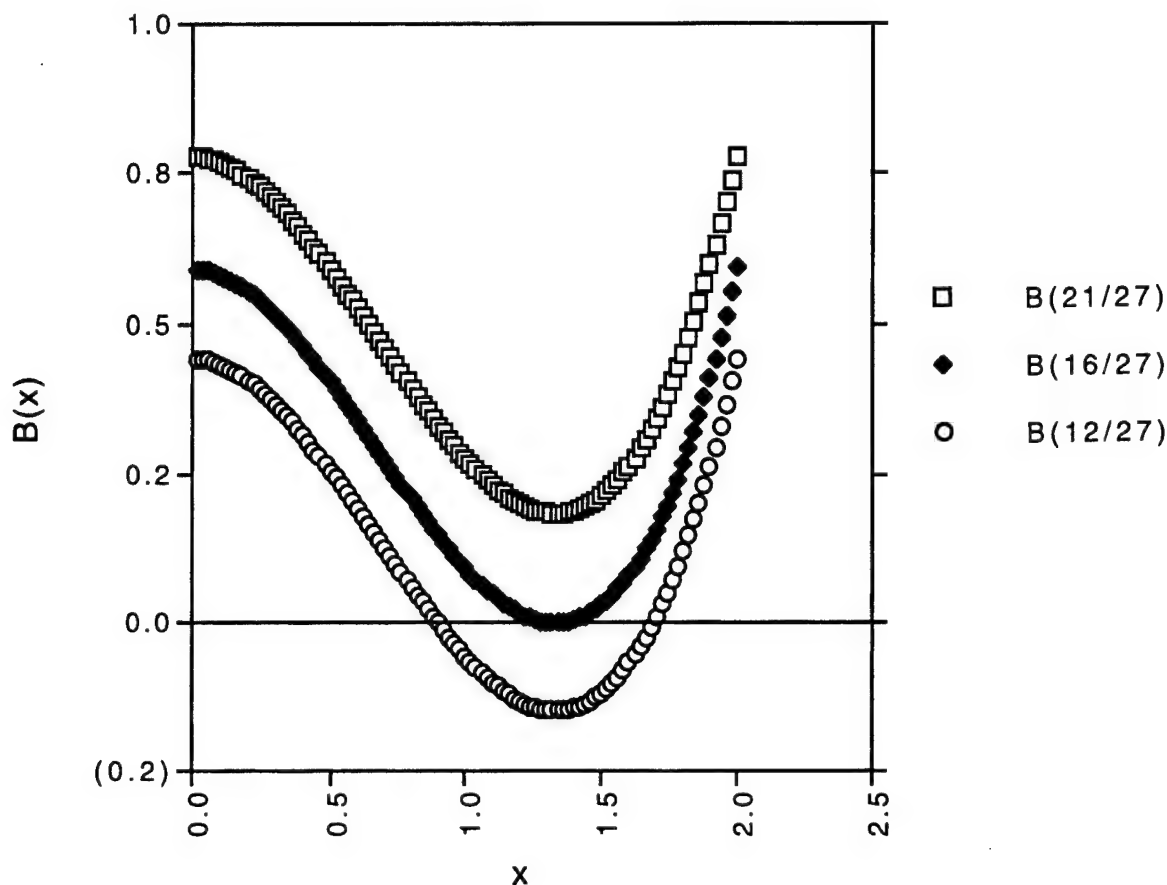
Figure 9
B(x) Versus x

2.3 Production of Atoms *In Situ*

Atoms, produced and trapped in solid hydrogen hosts, have been studied by a variety of experimental techniques but detailed knowledge is still quite fragmented. Admittedly, the experiments have all been complicated, but just a few clear results have been established for a system that has the potential for storing large quantities of energy (in the form of atoms).

2.3.1. Motivation for a New Model of Atom Production. Leach and Fitzsimmons [9] produced atoms of hydrogen in solid molecular hydrogen by bombarding the solid

26

with 160 keV pulsed electron beams. The electron pulses produced atoms in the solid that were then studied from the time decay of their distinctive ESR signal. From their estimates, 300 atoms were produced per 160 keV electron. Since the signal intensity is proportional to the number of atoms, they were able to conclude that the atom density decay followed:

$$(28) \qquad \frac{1}{n(t)} - \frac{1}{n(0)} = 2\alpha t$$

From which one deduces a rate equation for the atom density,

$$(29) \qquad \frac{dn}{dt} = - 2\alpha n^2$$

previously used and known as the bimolecular recombination equation, the one expected from a process involving two entities. In addition, they found that the recombination coefficient, 2α, was strongly temperature dependent, with an activation energy (195 K) that matched that of the self-diffusion coefficient of molecules in solid hydrogen. The lower the host temperature, the smaller the diffusion coefficient and hence the smaller the atomic recombination coefficient.

Prior to the Leach and Fitzsimmons work, Sharnoff & Pound [22] had made a careful study of solid deuterium that contained nominally 1% of tritium (T_2), again using ESR techniques to detect the D atoms produced by the tritium beta decay. Their atom density as obtained from their signal intensity grew, then saturated, then grew again, all at constant temperature. One would expect that atoms, continuously produced by the beta decays, would eventually reach a maximum population where additional growth tendencies would be balanced by recombination. The atom growth curve observed by Sharnoff and Pound has never been satisfactorily explained until this study. From Leach's work, there should be temperature dependence in both the growth curve and the final atom density because of temperature dependence of the recombination coefficient. Between 4 K and 1 K, Sharnoff and Pound did not observe any temperature dependence. Leach estimated that 23 atoms were produced per tritium beta decay in the Sharnoff and Pound experiment.

Webeler [18] studied H_2 containing small amounts of T_2 but he didn't use ESR techniques. He studied the heat released when atoms recombined in the host solid and attempted to quantify storage times for the energy resident in the trapped atoms, again produced by the tritium beta decay. Rosen [16] and Zeleznik [17] provided a more detailed analysis of the Webeler experiments. Rosen's approach is examined here.

In his most general approach, Rosen treated two types of atoms, mobile atoms, that were really ballistic and trapped atoms. Mobile atoms were produced by the beta decay of tritium with about 3 eV of kinetic energy and percolated through the lattice like thermal neutrons, eventually becoming trapped after traveling on the order of 1 mm. The trapping of the mobile atoms in the solid led to the second type of atom. While either

27

type of atom could contribute to the stored energy, the trapped atoms outnumbered the mobile atoms by a factor of $\approx 10^4$, based on Rosen's choice of parameters. Diffusion was considered but then discarded because it complicated the analysis and didn't seem to be required to explain the experiments. Estimates were made of all the pertinent parameters and recombination was treated by gas-phase calculations of the cross-section leading to a temperature-independent recombination coefficient ($2\alpha = 2.6 \times 10^{-15}$ cm^3/s) applicable to mobile atom — mobile atom events or mobile atom — trapped atom events. If an oversimplified version of Rosen's model is used, reduced to one type of atom, say the trapped atoms, the atom density would obey a rate equation given by Equation 20, where K_a would represent the constant atom production from tritium beta decays and would be roughly $2\alpha/10^4$. Rosen assumes that the atom density is uniform across the sample which, in turn, predicts a steady-state atom population given by $n_0{}^2 = K_a/\alpha$. This buildup, starting from $n = 0$, and saturation is shown in Figure 8, the curve without vacancy filling.

Although Rosen's model is valuable in understanding the heat released in Webeler's experiments and points out the critical role of the coupling between the sample and the refrigerator, there are several difficulties with it:

(1) the model vastly overestimates the volume within which the atoms are produced, because an H atom does not travel through solid hydrogen like a thermal neutron but thermalizes in a much shorter distance;

(2) there appears to be no mechanism for untrapping an atom since 3 eV would be required to convert a trapped atom into a mobile one; and

(3) the model cannot explain the observed temperature dependence of the many experiments on atoms in solid hydrogen, other than the Webeler experiment.

First, the recombination coefficient has been directly measured by Leach [9] in an experiment where the H atoms were produced by an electron gun and the ESR measurements were made with the beam turned off. He found that $\alpha = 6.0 \times 10^{-21}$ cm^3/s at 6.75 K and rapidly decreased with temperature. Russian data [10,11], where the H atoms were produced by trapping atoms formed in a microwave discharge, interpreted by Souers [24], would lead to values of $\alpha = 1.5 \times 10^{-24}$ cm^3/s at 2 K and $\alpha = 7.5 \times 10^{-25}$ cm^3/s at 1.4 K. It can be argued that both of these experiments are sensitive to the recombination of trapped atoms, not considered by Rosen. However, in the temperature range of interest in the Webeler experiments, the recombination used by Rosen differs from the estimates made in the solid state by at least 5 orders of magnitude. For a recombination coefficient of the magnitude used by Rosen, the calculated atom density from the heat observed in a triggered energy release could not be established for the atom production term he used.

Second, Rosen estimated the volume for trapping of atoms and multiplied that volume by the beta-decay rate to compare with the actual volume of the sample. Since his calculated volume per second receiving new mobile H atoms was comparable to the sample volume, he concluded that it was appropriate to consider the volumetric rate of production of mobile H to be approximately constant and uniform throughout the H$_2$

28

sample. In the new model, where the parameters are obtained from other experiments where possible, a much smaller critical volume (not a trapping volume) is obtained that leads to a small fraction of the sample receiving new atoms per second for the beta-decay rate appropriate to pure T_2 solid. In this case, it is not appropriate to consider the atom production to be uniform and atom production will be treated differently.

A new model is proposed that is simpler in some respects but more complicated in others, than Rosen's. This model attempts to explain the ESR experiments (that Rosen was not addressing) and draws on other experiments such as the measurements of the range of beta particles in solid hydrogen for its parameters.

The pertinent features of this new model are: (1) a new approach to atom production, where the solid is treated as consisting of regions with different atom densities, not a homogeneous medium, leading to a different time dependence of the atom density at fixed temperature; (2) a new interpretation of the ESR results is made possible; (3) the model has some predictive ability and can give an upper bound for the maximum atom density for a specified production process; (4) it predicts that the production term, used in the model, can depend on the materials properties of the host and possibly the temperature and not just the fraction of tritium in the sample; and (5) it can guide experiments attempting to make large atom densities by electron bombardment.

In the analysis of most of the experiments to date, the level of detail of the observations has not warranted using a theoretical picture with the (unphysical) complexity of Rosen's (i.e., two types of atoms) so previously the problem was treated as though only one type of atom existed. In trying to reconcile the atom densities obtained from a model analysis of ortho-para conversion times in T_2 (or DT) [25] with (1) measured atom densities in ESR experiments [26] and (2) the time dependence of the density after a temperature change (or heat spike) [27], it is apparent that the single type of atom model, with homogeneous production of atoms, that has been used is inadequate to explain the data.

The beta decay of a single tritium atom creates atoms in a restricted volume (a bubble) of the crystal. In this region, there can be a dramatic thermal response (local heating) and atom recombination. Atoms created in this bubble can recombine there or diffuse, enlarging the bubble. The critical initial bubble volume is estimated from the measured range of electrons in solid H_2 and a calculation of the distance traveled by a 20 eV secondary electron, making the bubble shape that of a long, thin cylinder. An effective atom production rate is obtained that depends on the temperature and the material. Application of this model to electron paramagnetic resonance experiments indicates that many atoms can go undetected in ESR measurements when the atom density is large. The bubble model is used to estimate the low temperature ortho to para conversion rate in solid tritium.

2.3.2. A New Model of Atom Production in Solid Hydrogen Hosts. Atoms can be produced *in situ* by electron bombardment of H_2 or by radioactive decay (beta decay) of tritium nuclei incorporated into the host solid (or even forming the host solid). In either case, the role of an electron is crucial. The motion of an electron injected into solid H_2 is complicated and can only be described in a statistical sense. Historically, this problem has

been the subject of interest to high energy physics but for electron energies much above those of interest for tritium beta decay or for the production of atoms in solid H_2.

A collision with a nucleus would lead to large angular deflection while a collision with another electron bound to a molecule could result in almost no angular deflection. The former situation leads to multiple Coulomb scattering and for electrons with energies of 400 keV, incident on solid argon, 10% of the energy is deposited behind the starting plane. For electrons incident on solid H_2, by the time the energy has fallen to 1.4 MeV, there has been a one radian deflection but this effect has not been quantified in H_2. The latter situation results in an accumulation, as the electron loses its energy, of a large number of small angular displacements. These, also, have not been quantified in solid H_2.

The approach followed differed from that of Rosen [16] in that the focus was on a single beta decay and its effect on the surrounding region of the solid. The region created by the beta decay was labeled a bubble and the sudden increase of energy available in this region may form a hot spot. A more careful treatment would take into account the actual spectrum of tritium beta-decay energies but only the decays characterized by the mean energy of 5.7 keV were considered.

The energy loss of an electron in matter has been successfully described by a continuous slowing down approximation where it is assumed that the electron has many collisions (380 for an initial energy of 5.7 keV) with the atomic electrons and multiple Coulomb scattering is ignored. Although the electron does not suffer that many collisions and it does not transfer its energy in very small (but nearly identical, 15 eV) bits, the predictions that emerge are consistent with the limited experimental observations. The prediction of the electron practical range in H_2 and its dependence on the initial electron kinetic energy is a good example.

For this initial energy, the trajectory of the electron is approximately straight but many secondary electrons are produced as the initial electron slows down. Accordingly, the region influenced by this electron (the bubble)is presumed to be a cylinder. One dimension of the bubble volume was chosen to be the practical range (L) of a 5.7 keV electron in solid hydrogen and the transverse dimension (R) was taken to be the range of a 20 eV secondary electron produced in large numbers from the energy loss of the primary beta electron.

Schou and Sorensen [28] measured the range (L) of electrons in H_2 and D_2 for initial kinetic energies (E) between 500 eV and 3000 eV by using thin films of hydrogen. They obtained the result that:

$$(30) \qquad\qquad L = \left(\frac{K}{\rho} \right) E^{1.72}$$

where K is a constant and ρ is the density (of H_2, D_2, or T_2). Thus an electron with initial energy of 5.7 keV would have a range in solid H_2 of 3.9 μm or in solid T_2 a range of 3.2 μm before losing all its energy. According to this picture, the electron would lose its energy in 15 eV increments and have about 380 collisions before stopping. In fact, the number of actual collisions could be much smaller.

The transverse dimension, the range (R_e), can be estimated from the known

stopping power formula. From Souers [24], $(dE/dx) = 5.21 \times 10^{-10}$ J/m, for 20 eV initial energy and with the choice of 5 eV as the typical (but arbitrary) energy loss per collision in the low energy range. Thus:

$$(31) \qquad\qquad R_e = \frac{\Delta E}{(dE/dx)} = \frac{5\ eV}{(0.328\ eV/\text{Å})} = 15.4\ \text{Å}$$

for H_2 and 12.5 Å for T_2 (because of the larger density). Doubling the energy loss per collision to the value more appropriate for dissociation doubles the range but will make no appreciable change in the estimates given by the bubble model, since the effective atom production rate depends only on the logarithm of the transverse dimension so that a factor of 3 error in R_e would produce only a 10% change in the rate.

Thus with these dimensions, the bubble is a long, thin cylinder. The volume of a bubble in T_2 with this radius (12.5 Å) and length 3.2 μm would be 1.57×10^{-17} cm^3, while the comparable volume in H_2 would be 2.9×10^{-17} cm^3. Given the beta decay rate of $R_\beta = 1.15 \times 10^{14}$ events/cm^3/s, in a pure T_2 sample of volume 1 cm^3, 1.8×10^{-3} cm^3 of new bubbles are created each second. For the 2% T_2 samples, such as those studied here, there are 3.6×10^{-5} cm^3 of new bubbles formed each second or in a sample of volume 1 cm^3, only 36 parts per million (ppm) of the sample would receive new atoms each second, justifying use of a model based on inhomogeneous atom production.

Since the bubble volume is so small, the thermal response could be unusual. The average beta particle leaves 5.7 keV in the bubble region while producing about 800 atoms, if the gas phase result is used for atom production. As soon as the atoms have thermalized, they store 400 times 4.5 eV or 1.8 keV, leaving 3.9 keV to be dissipated in the bubble and its vicinity.

The enthalpy of T_2 has been estimated from measurements and comparison with known values for H_2 and D_2. At the critical point, the enthalpy is 1500 J/mol (or 15.6 meV per molecule). If the above value is used for the cylinder volume, there are 5×10^5 molecules with the average molecule having 15.6 meV enthalpy at the triple point for a combined total of 311 eV. Thus if 3900 eV is deposited into a region containing 5×10^5 molecules (or 7.8 meV per molecule), the region will not reach the critical point. However, smaller estimates of the bubble volume are possible; for instance, one could assume the bubble volume is 400 times the volume of a sphere of radius 12.5 Å. This reduces the volume by a factor of 5 so that only 10^5 molecules are in the volume. In this case, there is enough deposited energy to reach (and exceed) the critical point. However, based on a classical analysis, the thermal relaxation of such a region would be unbelievably fast, on a time scale of 10^{-17} seconds, shorter than an optical phonon vibrational time. The new region might have very different characteristics than the original solid; it might not have the same long range order.

The experiments to date have been sensitive only to time scales of seconds to minutes. In a fraction of a second, all the atoms that are going to be produced because of a single beta decay have been produced and many have had the opportunity to recombine. Of those atoms remaining in the bubble, some diffuse away from the point where they

31

were created, enlarging the bubble. Subsequently, they can be detected in an electron spin resonance experiment. Those atoms that are counted in the detection process have their ESR frequency address located within a magnetic field window (ΔH) centered on the particular hyperfine-split line in question. This window depends on the signal-to-noise ratio and the sensitivity of the spectrometer. All the atoms created in the bubble do not instantly appear in the ESR signal; if they are located within two lattice sites of another atom, the ESR frequencies of both atoms will lie outside the detection window and will not be counted. Atoms produced in the high density regions of the bubble must then diffuse through space into regions of lower atom density, decreasing their local magnetic field and making them detectable.

To quantify these effects, a microscopic equation for the recombination time for the atoms, including the dependence of its variables on the material properties of the host, was developed. For two atoms to recombine, they first have to hop within a nearest neighbor distance of each other and then they must recombine. This last step may be decidedly nontrivial since the repulsive core for the H to H_2 potential is wider than that for the H_2 to H_2 potential. Thus there could be a substantial repulsion between atomic H nearest neighbors in the H_2 host. In any case, the average recombination time T for atoms is:

$$(32) \qquad T = \frac{\left(\dfrac{\xi_1 \tau_h}{Z} + \tau_r \right)}{Zc}$$

where ξ_1 is a numerical constant of order unity, Z is the number of nearest neighbors, and $1/\tau_r$ is the recombination rate for neighboring H atoms. The quantity $1/\tau_h$ is the probability per unit time for an H atom to hop a specific neighboring site and c is the concentration of atoms.

In the bubble of H atoms being considered there are N atoms in a volume V. Thus c, the concentration of atoms, is given by the equation

$$(33) \qquad c = \frac{N v_0}{V}$$

where v_0 is the volume of a cell containing one H_2 molecule. Thus V/v_0 is the number of unit cells or H_2 molecules in the bubble. The differential equation governing the decrease in the number of atoms in the bubble is

$$(34) \qquad \frac{dN}{dt} = -2 \frac{N}{T}$$

where the factor 2 obtains because each recombination destroys two atoms. Further, V ,

which appears in this equation though the factor c in the recombination time T, depends on time because of diffusion. This time dependence can be well approximated by the equation

(35)
$$V(t) = \pi\left(L_0 + \sqrt{2Dt}\right)\left(R_0 + \sqrt{2Dt}\right)^2$$

where L_0 is the length of a cylinder and R_0 is the cylinder radius. The physics of this equation is just that for a diffusion process $\langle x^2 \rangle = 2Dt$.

Combining these equations, the form to be solved can be written

(36)
$$\frac{1}{N^2}\frac{dN}{dt} = -2\frac{rv_0}{\tau_h V(t)}$$

where r is given by

(37)
$$r = \frac{Z^2\tau_h}{\left(\xi_1\tau_h + Z\tau_r\right)}$$

v_0 is the volume per particle, and V(t) is given by Equation 35.

Note that the recombination coefficient is given in terms of the parameters previously introduced as

(38)
$$\alpha = \frac{Z^2 v_0}{\left(\xi_1\tau_h + Z\tau_r\right)} = \frac{rv_0}{\tau_h}$$

Now Equation 36 is solved with the boundary condition that $N = N_0$ at time $t = 0$, yielding a solution that can be written as

(39)
$$\frac{N}{N_0} = \frac{1}{[1 + \beta h(y)]}$$

where h(y) is given by the equation;

(40)
$$h(y) = \frac{\left[\ln\left(\dfrac{1 + y - \epsilon y}{1 + y}\right) + \dfrac{\epsilon y}{(1 + y)}\right]}{\ln(1 - \epsilon) + \epsilon}$$

The parameter $y = sx$ where x is the dimensionless time;

$$(41) \qquad x = \sqrt{\frac{t}{\tau_h}}$$

and s = $2a/R_0$ depends on the shape. The parameter ϵ in Equation 40 is defined as $\epsilon = 1 - R_0/L_0$. In Equation 40, h(y) is zero for y = 0 and unity for y infinite.

The factor ß in Equation 39 is given by:

$$(42) \qquad \beta = \left(\frac{4rN_0v_0}{V(0)} \right) \left(\frac{\ln(1 - \epsilon) + \epsilon}{- s^2\epsilon^2} \right)$$

The first factor in the expression for ß depends on the initial concentration of atoms in the bubble but is shape independent, while the second does depend on the shape. For a long, thin cylinder, $\epsilon \approx 1$ and the expression for ß becomes:

$$(43) \qquad \beta \approx \left(\frac{12rN_0a}{\sqrt{2\pi}ZL_0} \right) \left[\ln\left(\frac{L_0}{R_0} \right) - 1 \right]$$

Besides the bubbles that are nucleated by beta decays, one will have a rather uniform background density made up of bubbles that have grown very large from the diffusion (and lost atoms due to recombination). A sensible but arbitrary way to divide things is to consider the atoms in a bubble to belong to the uniform background density when the atom density of the bubble is comparable to the background density. In this case, the evolution of atoms in the background density is described by Equation 20 but with an effective production constant.

From the above equations, one can immediately deduce the effective number of atoms that each beta decay produces. At times long compared to the time needed to diffuse across the bubble radius, $\tau_d = R_0^2 \, \tau_h/4a^2$, the number density of atoms in the bubble $N(t)/N_0$, is comparable to the uniform background density. Then one can consider the bubble should merge into the uniform background and its remaining atoms will be added to the uniform background. Note that almost all of the recombination happens within several diffusion times, τ_d. The number of atoms left is given by Equation 39 with h(y) equal to unity. Thus one obtains the equation

$$(44) \qquad \frac{N_{eff}}{N_0} = \frac{1}{1 + \beta}$$

This analysis also yields an effective production constant for Equation 10. The relevant equation is

(45)
$$K_{eff} = \frac{K}{1 + \beta}$$

This is the quantity that belongs in Equation 22 since only a fraction of the atoms survive long enough to be incorporated into the uniform background. The H_2 sample can be pictured as containing a rather uniform density of atoms (the background) along with some high density bubbles. As the number of atoms in a bubble decreases and (especially) as the volume of a bubble increases, the atom density of the bubble becomes comparable to the density of the uniform background. Thus the bubbles supply the uniform background with a rate constant that is adjusted because many of the atoms don't survive long enough to be incorporated into the uniform background. In this case, the appropriate production term is K_{eff}.

The dimensionless quantity ß is the key parameter in the above expression. Note that it is proportional to the number of initial atoms, as one might have expected, and it also depends on the bubble shape. Thus for example, one could imagine changing N_0 or $V(0)$ by slightly doping the H_2 and/or injecting electrons with a variety of incident energies.

The effective production constant is dependent on the material properties of the host (i.e. H, D, or T) and not just on the fraction of radioactive T atoms. Further, this constant can be temperature dependent if r is less than unity.

Two limits of the effective production term, the limit obtained when $\tau_h >> z \tau_r$ and the opposite limit obtained when $z \tau_r >> \tau_h$ are considered. (1) When the hopping time is much longer than the recombination time, $ß_{cyl}$ is evaluated by taking take $N_0 = 800$, the gas phase value, a = 3.75 Å for H_2, L_0 = 4 mm for H_2, and $R_0 = 12.5$ Å. Thus from Equation 43,

(46a)
$$\beta \simeq \left(\frac{12rN_0a}{\sqrt{2}\pi ZL_0} \right) \left[\ln\left(\frac{L_0}{R_0} \right) - 1 \right] = 0.119 \ r = 17.2$$

making $K_{eff} \approx K/20$.

(2) When, however, the recombination time dominates the problem,

(46b)
$$\beta \simeq \left(\frac{12rN_0a}{\sqrt{2}\pi ZL_0} \right) \left[\ln\left(\frac{L_0}{R_0} \right) - 1 \right] = 0.119 \ r = 1.43 \left(\frac{\tau_h}{\tau_r} \right)$$

Thus ß could be much less than unity and the effective production term would then be the actual atom production term. This possibility introduces an important temperature dependence and isotope dependence into the problem. It is estimated $\tau_h/\tau_r \approx \frac{1}{2}$ at 1.4 K, making ß = 0.7 and $K_{eff} \approx K/2$.

One can estimate the hopping times from the diffusion data and the recombination times from a calculation of the time needed to flip the spin of an atom adjacent to another

atom, a T_1 calculation. Two atoms with parallel spins are prohibited from recombining. While there may be difficulties in their becoming near neighbors in the lattice due to an effective repulsion, once they are near neighbors, they could recombine almost instantaneously on the timescale of the ESR experiments if their spins were antiparallel. Thus an estimate of the time required for a spin-flip of one of the atoms gives insight into the time constant τ_r, the recombination time.

Abragam [32] has estimated the transition probability per unit time, P, for such a spin-flip using a Raman process. At temperatures $T << \Theta$, where Θ is the Debye temperature, P is given by:

$$(47) \qquad\qquad P \approx 732.5 \left(\frac{81\ \pi}{2} \right) \left(\frac{F_2 \hbar}{mv^2} \right) \left(\frac{T}{\Theta} \right)^7 \Omega_D \qquad (in\ s^{-1})$$

where F_2 is proportional to the second derivative of the dipole-dipole energy, m is the atom mass, Ω_D is the Debye frequency, and v is the sound velocity. Rough estimates of this rate give for H atoms, $P = (1.35 \times 10^{-4}\ s^{-1})T^7$ so that $\tau_h > \tau_r$ to below 2 K.

From estimates of the model parameters, it is found that the initial concentration of atoms in a bubble is about 5%. Such a density of free electronic spins, at a temperature of about 4 K, randomly distributed, would represent an extremely interesting magnetic system. There are no existing studies of the magnetic behavior of such a system so the arguments below will be based on extrapolations of results from other experiments.

What are the implications for obtaining even greater atom densities? In one second, 1.15×10^{14} new bubbles per cm^3 are created, with each bubble initially having volume 6×10^{-19} cm^3. Thus a small fraction, 7×10^{-5}, of the sample, each second, receives new atoms. A bubble is incorporated into the uniform background in a time of order the diffusion time. For a diffusion time of 150 s (the estimate at 4 K for T_2), only 1% of the sample is in this high density phase. This suggests that it may be possible to achieve much higher atom densities in the solid host, but not higher, for the calculation based on beta decay in solid T_2, than the initial atom density of 5 %.

In the above analysis, it was assumed that a single electron of average energy of 5.7 keV can create 1000 atoms in a small volume (a bubble) estimated to be of order 6×10^{-19} cm^3. The bubble expands due to diffusion and atoms in the bubble recombine. When the atom density decreases by a factor of 10 from its initial value, only half of the atoms have recombined, the major effect being a volume increase by a factor of 5. Thus a maximum atom density of about 2% does not seem impossible.

To enhance the chances of obtaining such high densities, it seems that limiting the effects of recombination by increasing the applied magnetic field and possibly increasing the pressure are most likely to succeed. In the experiments of Smith and Squire [33] on solid molecular H$_2$, modest increases in the pressure (p = 1 atm to p = 230 atm) made significant increases in the activation energy (E_a = 175 ±25 K to E_a = 280 ±25 K) for diffusion and, by implication, the diffusion time. Without additional data, one cannot speculate on the modifications required for this bubble model due to changes in pressure and magnetic field.

2.4 H_2 Monolayers Absorbed on Activated Carbon Fibers

When the spins are confined to lattice positions, the NMR lineshape is essentially Gaussian in nature (Gaussian FID) and its width ($\Delta\omega$) is well characterized by the second moment, M_2, with ($\Delta\omega$) $\approx \sqrt{(M_2)}$. Time dependence (motion or spin flips) of the spins results in a narrower line and a change in lineshape from Gaussian to Lorentzian (exponential FID), effects predicted by Anderson and Weiss [31]. If the motional frequency is Γ, the motionally narrowed linewidth is given by: ($\Delta\omega$) $\approx (M_2)/\Gamma$, a result valid so long as $\Gamma > \sqrt{(M_2)}$. The motion responsible for this narrowing can come from actual translational hopping, in which case the data can be used to infer diffusion coefficients, or it can be caused by intramolecular interactions between neighboring oH_2 molecules that produce spin-flips, without any translational motion. These latter interactions are absent in pure HD so that a narrowed HD resonance line is indicative of translational hopping.

In experiments with pure HD (about 1.9% H_2 and 0.3% D_2), a Lorentzian lineshape was observed, indicative of motional narrowing, and the weakly temperature-dependent observed widths (2.2 x 10^4 at 13.6 K to 4.4 x 10^4 rad/s at 5 K) are smaller than the width predicted from the second moment (5 x 10^4 rad/s). This is shown in Figure 10. At 7.6 K, the hopping frequency calculated from the data is $\Gamma = 8$ x 10^4 rad/s and the 2-D diffusion coefficient is $D = <a^2>\Gamma/4 = 2.3$ x 10^{-11} cm^2/s, comparable to the 3-D value for H_2 at 11 K.
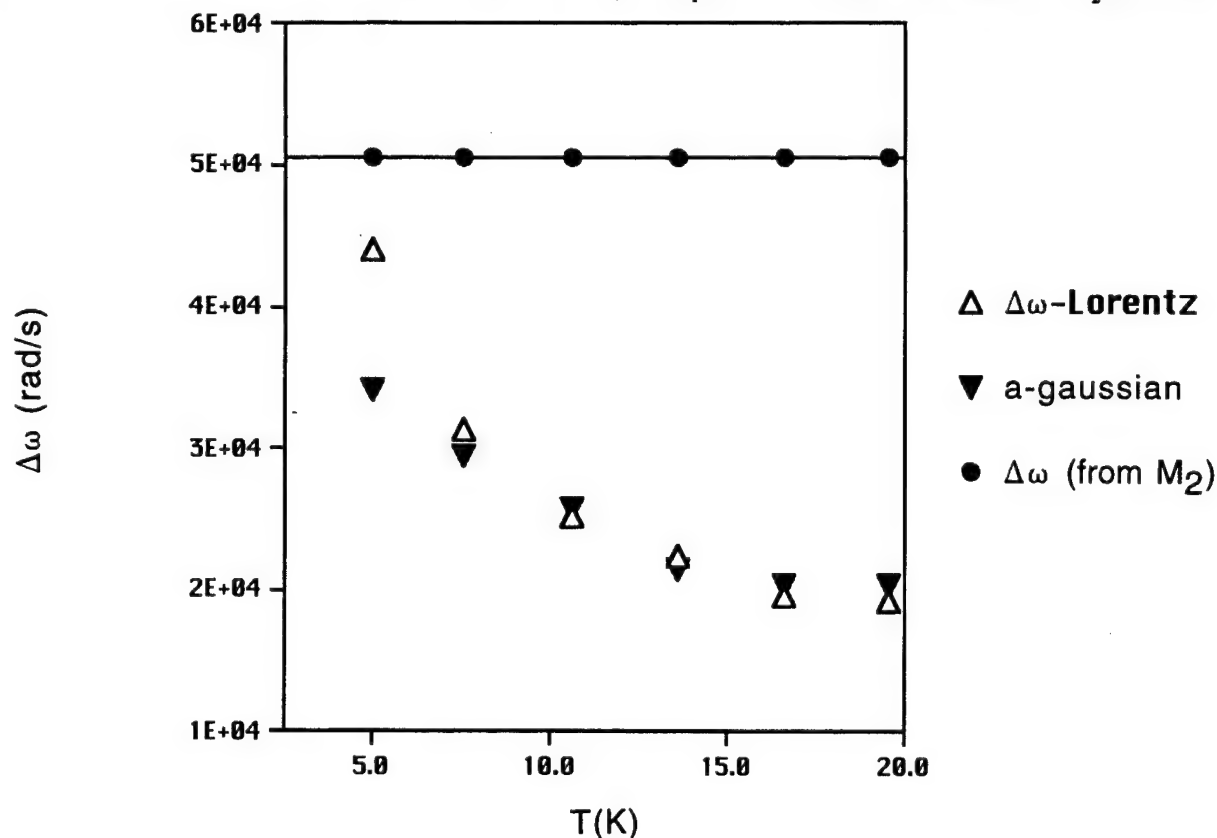

Figure 10
Linewidth versus T

The NMR lineshapes of H_2 molecules absorbed on ACF are also Lorentzian and, at the starting oH_2 concentration of $x_1 = 0.75$, all widths are narrower than predicted from the calculated value of M_2. As the samples age, at fixed temperature, their linewidths increase, exactly the opposite behavior expected from spins on a rigid lattice. This is shown in Figure 11.
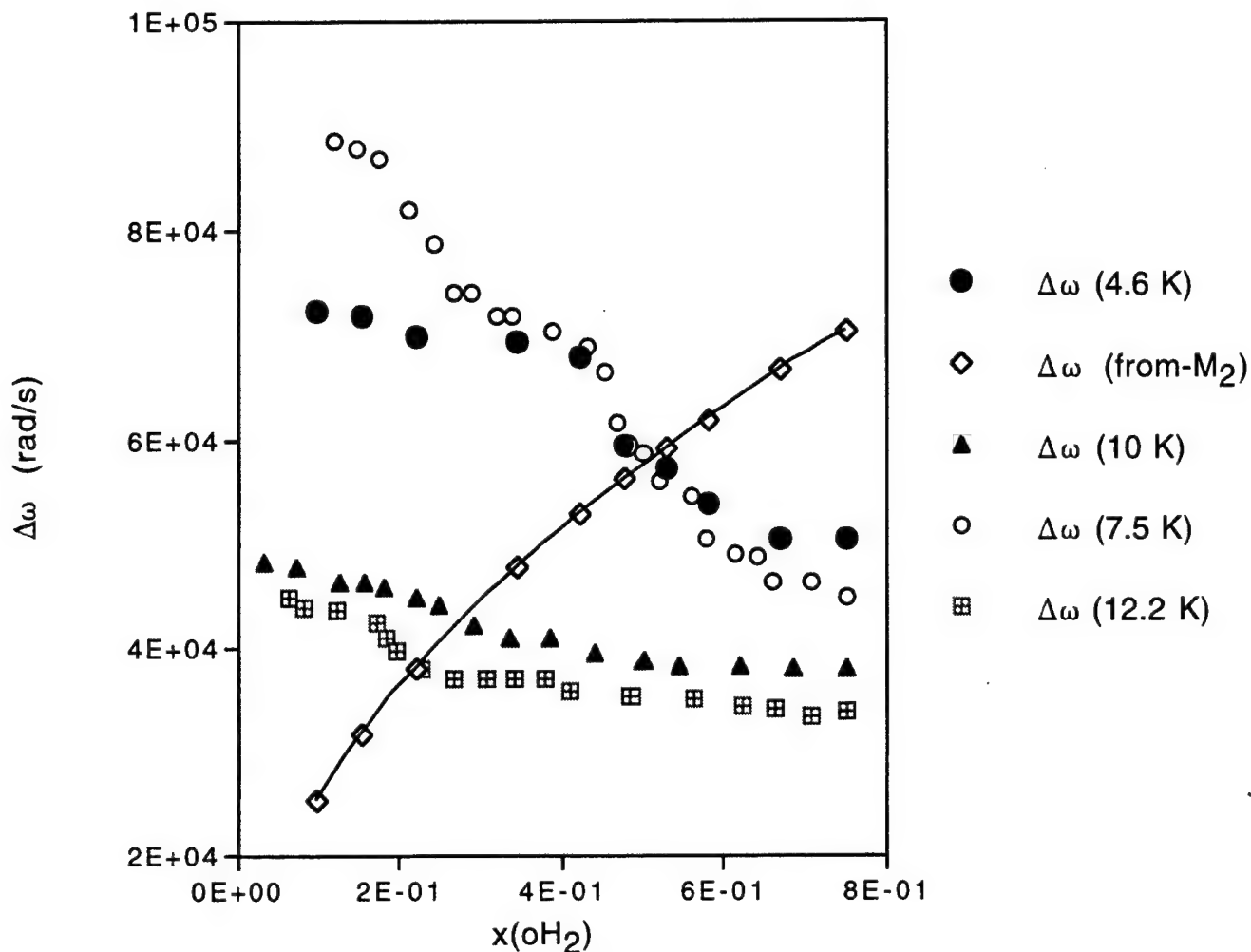

Figure 11
Linewidth Versus Ortho H_2 Concentration

This would indicate that the hopping frequency decreases with decreasing oH_2 concentration. Nevertheless, the hopping frequencies are comparable to those found in HD and the diffusion coefficients are of order of magnitude 10^{-11} cm^2/s. The weak temperature dependence of the hopping frequencies for $x_1 = 0.75$ is characteristic of an activation energy of 5 K.

Since the NMR signal height for H_2 is directly proportional to the number of oH_2 molecules, the decay of the signal at fixed temperature can be used to study the oH_2-pH_2 conversion process. Two types of conversion have been studied previously: intrinsic conversion where the intermolecular interaction between molecules provides the magnetic

38

field gradient needed for conversion and catalyzed conversion where a paramagnetic impurity such as an H (or O) atom or O_2 molecule provides the needed magnetic field gradient.

Using a strong collision approach to calculate the local transition probabilities, one obtains the following differential equations for intrinsic conversion:

(48)
$$(a)\frac{dN_1}{dt} = - (N_1)^2(\frac{Zv_0}{\tau})f_c \quad \text{if } W_{10}\tau > 1$$

$$(b)\frac{dN_1}{dt} = - (N_1)^2(Zv_0W_{10})f_c \quad \text{if } W_{10}\tau < 1$$

where $\tau(\tau = \Gamma^{-1})$ is the time to hop to any of the Z nearest neighbor sites, v_0 is the volume per particle such that $v_0N_T = 1$, and f_c is a correlation function that gives the fraction of near neighbor sites at the new site that were not near neighbor sites at the old site. For the hcp lattice, $v_0 = a^3/\sqrt{2}$. To modify this for 2-D, replace v_0 by A_0, the area per particle, where $A_0 = (\sqrt{3}/2)a^2$. For two dimensions f_c is approximately 0.50.

For intrinsic conversion, $(N_1)^{-1}$ is linear in time and the rate has been measured [32] for H_2 and found to be 1.9% per hour or 5.3×10^{-6} s^{-1}. A careful calculation of the basic rate in H_2 has been done [33] finding a rate of 1.67% per hour.

Using the same procedure as above, the differential equations for catalyzed conversion (with c_a the concentration of unpaired electron spins) were obtained:

(49)
$$(a)\frac{dN_1}{dt} = - (N_1) (\frac{Zc_a}{\tau})f_c \quad \text{if } W_c(a) \tau > 1$$

$$(b)\frac{dN_1}{dt} = - (N_1) (Zc_aW_c(a))f_c \quad \text{if } W_c(a) \tau < 1$$

In both cases, there is an exponential decay of the number of ortho molecules, $N_1(t) = N_1(0) \exp(-kt)$, where k depends on which of the above limits applies.

By using the factors in the calculation (but using the experimental value of the H_2 rate), it is possible to predict: the intrinsic conversion rate for an H_2 monolayer (2-D intrinsic rate $W_{10} \approx 1.7 \times 10^{-5}$ s^{-1}) and the transition probability per unit time due to an unpaired electron spin at the nearest neighbor spacing (a). For 3-D H_2, this is $W_c(a) = 5.46 \times 10^{-2}$ s^{-1} (in agreement with the estimate of Shevtsov, *et al.* [34]). This latter rate can be adjusted to the monolayer spacing giving for 2-D, ACF, the value $W_c(a)^{2-D} \approx 0.177$ s^{-1}. The measured oH_2-pH_2 conversion rates are about a factor of 10 larger than the predicted intrinsic conversion rates and the signal decay is approximately exponential, indicative of catalyzed conversion. This is not surprising since O_2 contamination of the surface is assured given the transport and handling conditions of the ACF. Thus intrinsic

39

conversion was ignored in the analysis here.

There is an additional feature to the time decay of the NMR signal at fixed temperature, namely, the conversion rate appears to increase rather abruptly with time, a phenomenon observed previously for 3-D bulk H_2 by Schmidt [32] at 1.57 K and by Rall, *et al.* [35] for H_2 absorbed on zeolite. This is shown in Figure 12.
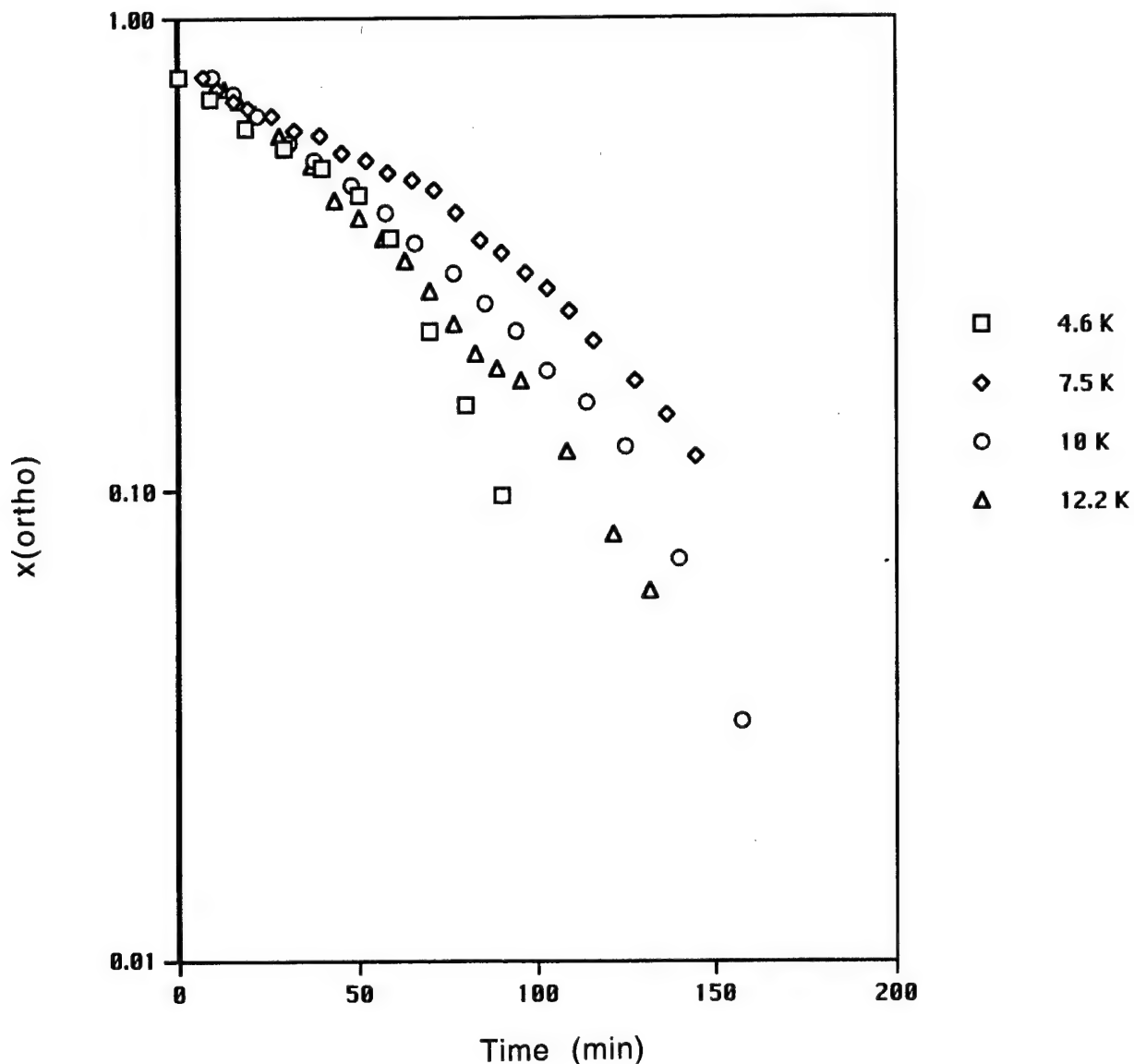

Figure 12
Ortho H_2 Concentration versus Time

In the fast diffusion limit, the rate k_1 is given in Equation 49b: $k_1 = Zf_c c_a W_c(a)$. For $Z = 6$, $f_c = 0.5$, and $W_c(a) = 0.177$ s^{-1}, it is obtained from $<k_1>$ that $c_a = 4 \times 10^{-4}$ (or 400 ppm). This limit implies that Γ is larger than 0.177 rad/s. Motionally narrowed NMR

40

lineshapes require Γ's larger than 10^4 rad/s.

In the slow diffusion regime, then $k_1 = Zf_c c_a \Gamma$ and the mean rate implies that the product $c_a \Gamma = 7 \times 10^{-5} s^{-1}$. c_a is not known independently but choosing $\Gamma \approx 10^4$ rad/s, consistent with the NMR line narrowing, would imply that $c_a \approx 10^{-8}$, an unlikely value (much too small for samples exposed to air in shipping). Thus it is concluded that the data is in the fast diffusion limit and the hopping frequencies can be determined from the NMR line narrowing but not the ortho-para conversion rates. The H_2 data is consistent with the HD data and yields diffusion coefficients on the order of $D \approx 10^{-11}$ cm^2/s.

There is no explanation for the increase in the conversion rate observed as the samples age at fixed temperature. Other workers [35,38] attributed the increase they observed to clustering of the ortho molecules driven by the electric quadrupole-quadrupole interaction. While this might be true for their experiments, it is not a likely source of increased conversion when the conversion is catalyzed by unpaired electron spins. From the NMR lineshape narrowing, there is no indication of increased diffusion as the samples age; rather the opposite is true. The frequency Γ appears to decrease (and hence D) with decreasing ortho concentration (x_1) or increasing age.

3.0 SUGGESTIONS FOR FUTURE WORK

The suggestions for future work are divided into three categories;
(1) conventional diffusion measurements but on vapor deposited solids, (2) non-conventional diffusion measurements that can pinpoint the actual molecule hopping time unambiguously at low temperatures, and (3) basic measurements of the spin-lattice relaxation time on HD and H_2 molecules in monolayers.

3.1 Conventional Diffusion Measurements

Additional measurements of the self diffusion coefficient, D, in vapor deposited hydrogen solids (a-H_2), from near the triple point temperature to the lowest practical temperatures using conventional NMR techniques, should be made. There is now comprehensive literature on these same measurements in solid H_2 prepared by crystallization of the liquid (c-H_2). Thus a comparison of the two sets of data will make it possible to quantify the differences in vacancy concentrations in the two types of H_2 samples.

3.2 Diffusion Measurements in the Rotating Frame

The direct connection between molecular motions and the linewidth and relaxation of magnetic systems provides one of the most powerful techniques known for studying molecular motion. Molecular motion, of the diffusive type, is characterized by a mean time a molecule resides at a given site between jumps, $\tau = 1/\Gamma$. For the conventional motional narrowing approach, one can measure τ as long as τ is less than $(T_2)_{RL}$. For typical hydrogen solids, $(T_2)_{RL}$ is determined by intermolecular dipolar interactions and is on the order of magnitude of 30 μs to 400 μs.

The alternate technique first discovered in 1964 by Slichter and co-workers [36, 37] extends the range of measurement of motional correlation times by many orders of magnitude, making molecular motion quantifiable when $\tau < T_1$, the spin-lattice relaxation time. By this extension, it is possible to observe hopping times as slow as one lattice site hop per hour. This extends the range of t measurements from 10^{-4} s to 10^2 or 10^3 s (or more), a factor of more than 10^6. This is just the extension needed to study ultra-slow molecular hops in solid H_2 in the temperature range of interest to the HEDM program.

Slichter, using spin-locking, performed an adiabatic demagnetization in the rotating frame of reference where typical NMR experiments are treated. From his analysis and experiments, he concluded that very slow motions could be detected when the motional correlation time τ_m was smaller than T_1.

This technique was applied to NMR experiments in H_2 by the Gaines group [38] and in D_2 by Meyer and co-workers [6]. In an elegant set of experiments, they were able to measure, by conventional means, the motional narrowing approach, τ's that ranged from 10^{-6} s to 2 x 10^{-4} s. However by measuring the relaxation time in the rotating frame of reference, they extended the measurements of τ from 1 ms to 10 s at temperatures as

low as 8.9 K in D_2. By a scaling argument, this would correspond to a temperature of 5.8 K in H_2. Since this new technique permits measurement of τ if $\tau < T_1$, it is important to work in solid hydrogen where the relaxation time T_1 is long.

It is possible however to obtain, without great difficulty, long relaxation times in solid HD since the HD molecules have no intrinsic relaxation mechanism of their own — they can only change their spin orientation if they have oH_2 molecules in their neighborhood, making cross-relaxation possible. There it is necessary to either purify the HD to remove oH_2 impurities (HD samples have been made here by double distillation to remove H_2 molecules) or to hold the HD sample at low temperatures for a few weeks and allow the oH_2 impurities to convert to pH_2, which pose no problem. In either case, it is possible to produce HD samples with T_1s of several hundred seconds.

Because HD molecules have a different quantum parameter, the temperature of 5 K in solid H_2 corresponds to a temperature of $(5 \text{ K})(250/197) = 6.3$ K in HD. Thus experiments on HD at 6.3 K will provide the needed information about the hopping times in H_2 down to 5 K.

3.3 Measurements of the NMR Relaxation Times in H_2 Monolayers

Both H_2 and HD molecules confined to a two-dimensional array, such as that found for monolayers on ACF, are in mixed rotational states. The HD molecules are no longer in a pure $J = 0$ ground state but have a significant $J = 1$ component; even the $p\text{-}H_2$ molecules are in a state that mixes the rotational states $J = 0$ and $J = 2$. This mixing of the states nullifies one of the major simplifications found in 3-D solid H_2, namely that only the oH_2 molecules $(J = 1)$ possess a non-zero average value for the electric quadrupole-quadrupole moment.

Because of the mixed states in 2-D H_2, there must be measurements of the spin-lattice relaxation times in both HD and H_2 to understand the basic interactions between molecules on these surfaces. It is entirely possible that the motional narrowing interpretation used to deduce the diffusion coefficients of HD and H_2 molecules in monolayers on ACF is incorrect and that the observed effect is due to the electric quadrupole-quadrupole interactions between the molecules and not to molecular hopping.

4.0 CONCLUSIONS

New measurements of the molecular diffusion coefficient in HD, D-T, and T_2 solids were provided and the new data was interpreted, along with previous NMR and EPR data to extract both molecule and atom hop frequencies in the hydrogen isotopes. The vacancy exchange mechanism is responsible for both self diffusion of molecules and that of atoms. Based on this data and analysis, the following specific conclusions can be made.

Diffusion in these crystalline solids (c-H_2, etc.) is controlled by the number of vacancies in the lattice. This is in agreement with the theory of diffusion in hydrogen by Ebner and Sung [8] . The non-radioactive isotopes, H_2, HD, and D_2, have values of D_0 that are very regular and predictable from the relationship $D_0 = (0.0241)\Lambda^{-3.6}$. The radioactive isotopes have much larger values of D_0 that compensate, in part, for their much larger activation energies. The apparent activation energies may arise from lattice damage caused by the radioactivity that acts to suppress hopping and diffusion.

Values of the vacancy formation energy, E_v, the barrier height energy, E_b, and the energy of the first tunneling level in the hydrogen potential, E_t, defined by Ebner and Sung, have been estimated for all the isotopes. The activation energy according to the Ebner and Sung theory is given by: $E_a = E_v + E_b - E_t$. Model dependent values for these quantities have been given.

The values for the microscopic hopping rates of the molecules were obtained from the data. The vacancy hopping rate, at the triple point, for all the isotopes was calculated and found to be essentially the same for all isotopes. The microscopic atom hopping rates for crystalline samples are slightly larger, but nearly identical, to the corresponding hopping rates for molecules. Thus by studying the molecule hopping rates (say via NMR measurements) one can infer the atom hopping rates.

The recombination coefficients (and hence hopping rates) for crystalline solids differ from those of amorphous solids. Extrapolation of the data on crystalline solids to higher temperatures shows that atom diffusion is also dominated by vacancies and that at the triple point the atom hop frequency is somewhat larger than the molecule hop frequency.

One method of recombination suppression explains the bizarre features of the buildup curve, possibly pointing the way to storing much larger densities of atoms in solid hydrogen. It forms the basis for explaining the spontaneous heat spikes that occur at low temperatures when the atom density exceeds some critical value.

Thus the atom concentration obtainable depends on the initial vacancy concentration. Comparison of a-H_2 and c-H_2 results could test this prediction. Only when B(x) has no turning point can the value of x exceed the minimum in the curve B(x) that occurs at x = 4/3 and produce an atom buildup curve like that seen in 1963 by Sharnoff and Pound [22] and more recently by Collins [23]. Sharnoff and Pound observed D_2 containing 1% T_2 while Collins studied H_2, HD, and D_2 containing 2% T_2. Note that at the critical point, the saturation value of x if there was no correction for vacancy filling would be 0.770 rather than 4/3. Thus the saturation level is higher by a factor of $1.732 = \sqrt{(3)}$.

The problem of atom production in a solid hydrogen host containing tritium was reformulated in terms of a local, inhomogeneous, production of atoms that can then

diffuse into the bulk of the solid, forming a uniform background.

The basic unit in the model is a bubble that contains all the atoms created by a single beta decay. After creation of the bubble, two effects are considered: the boundary expands due to atom diffusion and atoms can recombine. There is no flux of atoms across the bubble boundary. To estimate the initial size of the bubble, an extrapolation of the measured range of electrons in solid hydrogen and an estimate of the distance traveled by 20 eV secondary electrons is used. The size estimate is that 800 atoms are produced in a region occupied by 5×10^5 molecules.

The bubble, small in size initially, contains atom densities higher than ever observed before in a hydrogen host. The time constant that characterizes the lifetime of the bubbles is the diffusion time, τ_d. In that time, the atom density decreases by a factor of approximately 10, the reduction coming from recombination and expansion caused by diffusion, with expansion making the dominant contribution. The initial high atom density results in spins that are unobservable by EPR and negates the use of EPR experiments to determine the number of atoms in a hydrogen host. The spins that are observed are free spins, not necessarily characteristic of the other spins in the solid and cannot be used to determine directly the population of spins.

Through analysis of the bubble geometry, a phenomenological theory that explains and brings together various pieces of data has been provided. This includes the materials dependence of K_{eff}, the data of Collins, *et al.* [14] and addresses the concept of the missing spins. It also gives a framework and mathematical model that one can push further. There are many complications that were ignored that are only appropriate for a much more sophisticated model. This includes the exact nature of the damage done by the atom formation, the heat, and possible nonequilibrium density of defects. In addition, the formulations of the missing spins arguments always start from initial random distributions of spins. This may not be justified at all.

Atom densities on the order of 2% seem possible if the atoms can be produced uniformly over the sample volume. A significant reduction in the recombination coefficient resulting from increased pressure, vacancy filling by atoms, isotopically substituted and disordered samples, or a large applied magnetic field could result in even higher steady-state atom densities.

In work on samples confined to two dimensions, estimates of the molecular diffusion coefficient can be made. The data is in the fast diffusion limit and the hopping frequencies can be determined from the NMR line narrowing but not the ortho-para conversion rates. The H_2 data is consistent with the HD data and each set yields diffusion coefficients of order $D \approx 10^{-11}$ cm^2/s.

There is no explanation for the increase in the conversion rate observed as the samples age at fixed temperature. Other workers attributed the increase they observed to clustering of the ortho molecules driven by the electric quadrupole-quadrupole interaction. While this might be true for their experiments, it is not a likely source of increased conversion when the conversion is catalyzed by unpaired electron spins. From the NMR lineshape narrowing, there is no indication of increased diffusion as the samples age; rather the opposite is true. The frequency Γ appears to decrease (and hence D) with decreasing ortho concentration (x_1) or increasing age.

5.0 REFERENCES

1. M. Bloom, *Physica*, 23, 767 (1957).

2. W.P. Haas, N.J. Poulis, and J.J.W. Bonleffs, *Physica*, 27, 1037 (1961).

3. F. Weinhaus and H. Meyer, *Phys. Rev.*, B7, 2974 (1973).

4. M. Rall, D. Zhou, E.G. Kisvarsanyi, and N.S. Sullivan, *Phys. Rev.*, B45, 2800 (1992).

5. F. Weinhaus, S.M. Myers, B. Maraviglia, and H. Meyer, *Phys. Rev.*, B3, 626 (1971).

6. F. Weinhaus, H. Meyer, S.M. Myers, and A.B. Harris, *Phys. Rev.*, B7, 2960 (1973).

7. R. Wang, M. Smith, and David White, *J. Chem. Phys.*, 55, 2661 (1971).

8. C. Ebner and C.C. Sung, *Phys. Rev.*, A5, 2625 (1972).

9. R.K. Leach, "A Paramagnetic Resonance Study of Hydrogen Atom Production and Recombination in Solid H_2 from 1.4 to 8 K," Ph. D. thesis, University of Wisconsin, Madison, Wis. (1972). University Microfilms, Ann Arbor, Mich. 48106, 1972, No. 72-23060.

10. A.Y. Katunin *et al*, Soviet Phys. *J.E.T.P. Lett.*, 34, 357 (1981).

11. A.V. Ivliev *et al*, Soviet Phys. *J.E.T.P. Lett.*, 36, 472 (1982).

12. P. Clark Souers, Hydrogen Properties for Fusion Energy, University of California Press, 1986, pp. 284-8.

13. J.R. Gaines, J.D. Sater, E.M. Fearon, P.C. Souers, F.E. McMurphy, and E.R. Mapoles, *Phys. Rev.*, B37, 1482 (1988).

14. G.W. Collins, P.C. Souers, E.M. Fearon, E.R. Mapoles, R.T. Tsugawa, and J.R. Gaines, *Phys. Rev.*, B41, 1816 (1990).

15. P. Clark Souers, Hydrogen Properties for Fusion Energy, University of California Press, 1986, pp. 10 ff.

16. Gerald Rosen, *J. Chem. Phys.*, 65, 1735 (1976) and 66, 5423 (1977).

17. Frank J. Zeleznik, *J. Chem. Phys.*, 65, 4492 (1976).

18. R.W.H. Webeler, *J. Chem. Phys.*, 64, 2253 (1976).

19. O.F. Sankey and P.A. Fedders, *Phys. Rev.*, B20, 39 (1979); Dieter Wolf, Phys. Rev. B10, 2710 (1974).

20. T. Moriya and K. Motizuki, *Progr. Theoret. Phys.*, (Kyoto) 18, 183 (1957).

21. I.F. Silvera, A. Driessen, and J.A. de Waal, *Physics Letters*, 68A, 207 (1978).

22. M. Sharnoff and R.V. Pound, *Phys. Rev.*, 132, 1003 (1963).

23. Gilbert W. Collins, Ph. D. Thesis, "A Magnetic Resonance Study of Atomic Excitations in Solid Hydrogen," The Ohio State University (1989).

24. P. Clark Souers, Hydrogen Properties for Fusion Energy, University of California Press 1986, pp. 284 ff.

25. J.R. Gaines, J.D. Sater, Evelyn Fearon, P.C. Souers, Fred E. McMurphy, and Evan R. Mapoles, *Phys. Rev. Lett.*, 59, 563 (1987).

26. G.W. Collins, P.C. Souers, E.M. Fearon, E.R, Mapoles, R.T. Tsugawa and J.R. Gaines, *Phys. Rev.*, B41, 1816 (1990).

27. G.W. Collins, E.M. Fearon, J.L. Maienschein, E.R. Mapoles, R.T. Tsugawa, P.C. Souers, and J.R. Gaines. *Phys. Rev. Lett.*, 65, 444 (1990).

28. J. Schou and H. Sorensen, *J. Appl. Phys.*, 49, 816 (1978).

29. A. Abragam, Principles of Nuclear Magnetism, Oxford University Press, 1961, pp. 401 ff.

30. G.W. Smith and C.F. Squire, *Phys. Rev.*, 111, 188 (1958).

31. P.W. Anderson and P.R. Weiss, Rev. Mod. Phys. 25, 269 (1953). There is a very clear description of this work in Principles of Nuclear Magnetism by A. Abragam, Oxford University Press 1961, pp. 447 ff.

32. F. Schmidt, *Phys. Rev.*, B10, 4480 (1974).

33. A.J. Berlinsky and W. N. Hardy, *Phys. Rev.*, B8, 5013 (1973).

34. Shevtsov *et al*, *J. Low Temp. Phys.*, 95, 815 (1994).

35. M. Rall, J.P. Brison, and N.S. Sullivan *et al*, *Phys. Rev.*, B44, 9932 (1991).

36. Charles P. Slichter and David Ailion, *Phys. Rev.*, 135, A1099 (1964).

37. C. P. Slichter, <u>Principles of Magnetic Resonance</u>, Springer-Verlag Berlin, 1980, p. 214 ff.

38. J.R. Gaines, Y.C. Shi, and J.H. Constable, *Phys. Rev.*, B17, 1028 (1978).